ITEP-5-02

Institute for Theoretical
and Experimental Physics

5 – 02

T.V.Kulevoy, R.P. Kuibida, V.A. Batalin
V.I.Pershin, S.V. Petrenko, D.N. Seleznev,
A.V. Kozlov, Yu.B. Stasevich, A.A. Kolomiets

STATUS
OF E-MEVVA ION SOURCE
EXPERIMENTS in 2000-2001 YEARS

Moscow 2002

УДК 621.387.324 М – 16

STATUS OF E-MEVVA ION SOURCE EXPERIMENTS in 2000-2001 YEARS
Preprint ITEP 5 – 02/
T.V.Kulevoy, R.P. Kuibeda V, .A. Batalin V.I.Pershin, S.V. Petrenko, D.N. Seleznev, A.V. Kozlov, Yu.B. Stasevich, A.A. Kolomiets – M., 2002 – 55 p.

The idea to use the independent electron beam to increase the charge states of ions in MEVVA discharge plasma was suggested in ITEP several years ago. We present the construction of latest version of MEVVA ion source with additional e-beam (e-MEVVA). The results obtained at this version of ion source clearly confirms the basic idea.

СТАТУС ЭКСПЕРИМЕНТАЛЬНЫХ РАБОТ НА ИСТОЧНИКЕ E-MEVVA В 2000 – 2001 гг.
Т.В. Кулевой, Р.П. Куйбида, В.А. Баталин, В.И. Першин, С.В. Петренко, Д.Н. Селезнев, А.А. Коломиец

Идея использования внешнего электронного пучка для повышения зарядового состояния ионов в плазме вакуумно-дугового разряда была предложена в ИТЕФ несколько лет назад. Представлена конструкция последней версии вакуумно-дугового источника ионов с внешним пучком (e-MEVVA). Полученные на данной версии источника результаты полностью подтверждают основополагающую идею источника.

Fig. – 37, ref. – 14 names.

© Институт теоретической и экспериментальной физики, 2002

Introduction

Metal Vapor Vacuum Arc (MEVVA) ion sources [1] are used to generate high current pulsed ion beams for both fundamental [2] and applied [3] research. The MEVVA is a prolific generator of highly ionized metal plasma from which metallic ions are extracted. A generic MEVVA [1] consists of a series of electrodes (usually concentric) that are separated by ceramic insulators. The commonly used configuration is a solid electrode of the desired metal, followed by a trigger electrode, an anode, a suppressor, and a three-grid extractor. Triggering of the vacuum arc is accomplished by applying a short high voltage pulse between the trigger electrode and the cathode across an insulating surface. Discharge occurs due to formation of cathode spots, which are micron-sized spots on the cathode surface characterized by extremely high current densities. Cathode material is vaporized and ionized, producing a plasma plume, from which ions are extracted. Although a MEVVA plasma is characterized by a high degree of ionization, only low ion charge states are typically produced. Depending on the cathode material used a conventional MEVVA ion beam has a mean charge state of about 2+.

For many applications [2,3] it is highly desirable to enhance the MEVVA ion charge state so that the ion beam energy can be increased without applying higher extraction voltage. Previous efforts demonstrated that the mean ion charge state in vacuum arc plasmas could be increased in a strong magnetic field [4,5], with high arc current [5], or by applying an additional short current "spike" on top of the main arc current [6]. Most previous attempts to obtain higher charge states quickly reached saturation [7] at charge states only 1.5 to 2 times higher than the conventional MEVVA. However, one promising approach is to attempt ion charge state enhancement using an energetic electron beam.

Over 30 years ago Donets invented the Electron Beam Ion Source (EBIS) [8], in which a high-energy, high-density electron beam produces multiple ionization of gaseous ions. Later, Batalin, et al. [9] combined an electron beam, a vacuum arc ion source, and a drift tube into a source called E-MEVVA, which produced encouraging indications of higher charge state production. Then, Hershcovitch, et al. [10] extended this concept using a Z-discharge plasma to generate an internal electron beam. With a gold cathode this Z-MEVVA gave results with some indication of charge states as high as Au 6+ . The E-MEVVA concept is obviously promising, but clear experimental proof of substantially increasing ion charge states remained elusive until the present study.

The project reported was aimed to join efforts from three research groups having the most experience with conventional vacuum arc ion sources for heavy ion,

plasma cathode electron guns, E-MEVVA and Z-MEVVA ion sources. They are ion source group of Institute for Theoretical and Experimental Physics, Moscow, plasma sources group of High Current Electronics Institute, Tomsk, both Russian and research group under the leadership of Dr. A. Hershcovitch from Brookhaven National Laboratory. Here we present experimental results obtained jointly in Moscow and concerning influence of the electron beam on charge state distribution (CSD) for the E-MEVVA ion source.

The e-gun investigation under operation with different type of cathode

The key point of e-MEVVA ion source is a producing of e-beam with high current density and energy of 5 – 20 keV. The fiber, plasma and semiconductor cathodes installed in e-gun have been investigated. Layout of e-gun with fiber cathode is shown in Fig.1 The distance of 2-3 mm between fiber cathode surface and opposite electrode (under 3 - 8 kV) has been chosen to provide the electric field at the cathode surface more than 20 kV/cm. This value has been used in experiments described in [11]. We did not obtain any e-beam current at the output of e-gun with fiber cathode. Moreover, the cathode has been destroyed after one hour of operation with repetition rate of 1 shot per 6 seconds. The discharge current and the voltage between cathode and opposite electrode have been measured. The typical results are shown in Fig.2.. One can see that the voltage drop is about 30 V and current is about 400 amperes. These values are typical for vacuum discharge between electrodes. To increase the lifetime of cathode, it is necessary to decrease the current through the cathode. Then we decreased the current in cathode circuit as down as possible (by installation of 2 kOm resistor). Anyway, if the breakdown is absent, the e-beam current is not detected at the e-gun output. For breakdown with the lowest discharge current of 1.5 ampere, the voltage drop is about 100 V. The result measured is shown in Fig.3. During this measurement, the cathode point was grounded and the voltage divider was reversed.

Layout of the e-gun with semiconductor cathode is shown in Fig.4. The polarity of electrical connection to electrodes clamped semiconductor is determined by the mechanical construction of diode used for cathode fabrication. At the axis of semiconductor, the aperture throughout the semiconductor body has been prepared. The gap of 2-3 mm between semiconductor surface and anode was standard for all our previous experiments. Therefore, the same distance has been used in described experiments. The e-beam current pulse of several amperes and length of 10-15 microseconds have been measured by beam transformer (BT). Also the current in cathode circuit and anode-cathode voltage drop have been measured. The results are shown in Fig.5. Again the voltage drop of 100 V for cathode current of 250 A are measured. Therefore, one can suppose that the vacuum breakdown occurs and e-beam is extracted from discharge plasma boundary.

Layout of e-gun with plasma cathode is shown in Fig.6. The construction of e-gun is the same as for the one with semiconductor cathode. The only one difference

is that the ceramic insulator is installed instead of semiconductor. The axial aperture with 1 mm diameter has been prepared in ceramic insulator. Such aperture diameter has been chosen to make the geometry of this e-gun similar to the one with semiconductor cathode. Therefore, the common MEVVA design is used as the e-gun. Below we will call such cathode as "ceramic cathode". The gap between anode and cathode of 2-3 mm has been used for this type of cathode as well as for other types. The anode-cathode voltage drop and cathode current have been measured. The typical results shown in Fig.7. The voltage drop of 50 V with current of 400 A has been measured.

We can conclude that for every type of the cathodes the electrons are extracted from boundary of plasma generated in e-gun. According to this conclusion, the ceramic cathode has been chosen for following measurements as the most reliable.

Magnet analyzer for CSD measurements

A new magnet analyzer was installed at the output of ion source, to provide the CSD measurements. Magnet analyzer photo is shown in Figure 8. Main parameters of it are given in Table 1.

Table 1. Parameters of magnet analyzer.

Bending angle	60°
Magnetic field range	0.1 – 1 T
Bending radius	0.3 м
Minimal step of magnetic field changing	$3*10^{-4}$ T
Width of magnetic field	3 см
Magnetic gap length	2 см

For ion beam collimation, two vertical slits of 2 mm width are installed at the input of the analyzer. The distance between them is 180 mm. As it will be shown forth, that system enables separate isotopes of copper ions – Cu_{63} and Cu_{65}. In order to increase the sensitivity of measured system, the one of this slit was taken out. As result the resolution of system is reduced but for most important experiments it does not significant. Especially if ion beam of heavy and low charged ions is investigated. As it will be shown forth, ions of Pb^{2+}, Pb^{3+}, Pb^{4+} can be easily identified in CSD measured with one slit.

At the MA output, the plate located behind the 2 mm slit is used as detector. Between slit and plate, the electrical field accelerating secondary electrons from measuring plate is used. It is done to increase the sensitivity of the detector. The coefficient of secondary electron emission can be different for different kind of ions. Nevertheless, this effect is not principle because the main goal of experiments was to find changing of peak amplitude for definite ions.

Measurements of ion beam CSD generated by e-MEVVA basic version with short e-beam

During all our previous experiments, the e-gun insertion leads to the appearance of "valley" in extracted ion beam. Therefore, the set of measurements with e-MEVVA has been started from tuning the ion source operation mode to have this "valley". The valley obtained for operation mode used during the measurements is shown in Fig.9. As it was described earlier [12] this effect indicates that some changes in CSD take place. These changes appear after the valley. Therefore we have been measured separately two regions in ion beam pulse – one is a region before the beginning of valley and second includes the valley region and region after it.

The main interest of measurements is to compare the CSD measured for e-MEVVA operated under two different modes – "with" and "without" e-beam. The magnet measurements for pulse ion beam especially with some instability in the charge states distribution require the long time. To provide the same operation condition during measurements for these two different modes, the following procedure has been chosen. For every magnetic field the signal from FC has been measured first for "with" operation mode and then for "without" one. As it was said previously for "with" mode two regions have been measured separately – one before the valley and second after it (see Fig.9). To increase the sensitivity of measurements, the dc negative potential has been applied to the measuring Faraday Cap. The measured signal has been picked off through the capacitors. Therefore the some amplification of detected signal (thanks to secondary electrons emission) has been obtained. In this way the peaks from measured CSD indicate the presence of ions with corresponding specific mass only. To use them for quantity calculation of ions distribution into beam, it is necessary to take into account the emission of secondary electrons for ions with different mass and energy. The results of measurements are shown in Fig.10. It is necessary to note the high resolution of the spectrometer. The isotopes of cupper Cu_{63} and Cu_{65} measured separately up to third charge state. The magnet measurements show the presence of U^{6+} ions into the beam. It is necessary to note that such kind of ions previously have been detected only when both the strong magnetic field (about 1T) and high discharge current have been used [13]. The magnetic field along plasma drift channel of e-MEVVA is 0.02 T. Nevertheless these ions have been detected in beam independent of e-beam presence. It is necessary to note that to supply the potential at the drift channel, the capacitor with small inner induction (2μF charged up to 300V) is used. It has been found that MEVVA discharge switch over to the drift channel wall and the discharge current rises to 300 A. Also this capacitor provides significantly increasing of the output ion beam current. The high amplitude of peaks corresponding to oxygen, carbon and other "dirty" ions can be explained by the fact that some vacuum accident happened and vapor of pumps oil is present in aria. It is

necessary to note, when the similar capacitors of 0.2 μF was used, the ions U^{6+} were not detected in generated ion beam.

Experiments with long e-beam

All investigations described above have been carried out with e-beam pulse length shorter than the discharge pulse length. To investigate the opposite situation, when discharge pulse length is shorter than the e-beam one, the triggering pulse of MEVVA has been used only. Its' length is 10 μs and can be decreased to 5 μs. The e-beam pulse length is not longer than 15 μs. The main result of experiment is that the ion beam current extracted from ion source falls down so much that both TOF method and magnet analyzer could detect nothing.

Assembling and tuning of new e-MEVVA design

On the base of the experiments with basic version of e-MEVVA it was concluded that it was necessary to upgrade coil at plasma drift channel to provide higher magnetic field. Also the new construction of MEVVA plasma generation had to be constructed to minimize the length of e-beam drift gap between e-gun and MEVVA discharge aria. As well the additional coil for magnetic field in this gap had to be constructed. New magnetic coils and MEVVA design have been manufactured and been installed instead the old ones. The magnetic field along plasma drift channel can be varied from 0.2 T to 1,5 T. That value is two orders more than field in old design. The coil for e-beam provides magnetic field up to 0.3 T at the axis. The magnetic field is matched to transport the e-beam from Tomsk e-gun to plasma drift channel. The electrical layouts for both coils are shown in Appendix.

On the base of experiments with basic version of e-MEVVA, it was concluded that it is necessary to design and manufacture the new version of MEVVA generator for this ion source. This design has to provide the shortest length of e-beam drift space between e-gun and plasma aria. Such new MEVVA plasma generated was designed and manufactured. The design of new MEVVA plasma generator is shown in Fig.11. The main parts of ion source are – cathode flange (pos. 3), cathode support (4) with cathode (10), insulator with conical hole (5), trigger (6), anode (7). The main aim of new design was to bring the MEVVA discharge aria close to input aperture for e-beam. In old design of MEVVA plasma generator the e-beam had to pass a drift space with length of 170 mm between input aperture and discharge aria. Only the e-beam charge space compensation provided the transportation of e-beam. The length of e-beam drift space in new construction is less than 40 mm. In final design, it is 30 mm. To keep the distance between the MEVVA anode (7) and plasma drift channel (9) as it was in old design, the additional tube was installed (8). The initial geometric parameters – diameters of halls in all electrodes and distance between them were the same as in old MEVVA design. As it will be described force, the diameters of halls in cathode, insulator, anode and additional tube (9) were

increased. In final design the cathode hole diameter is 12 mm. It follows the changing of halls' diameters in insulator and in trigger electrode. Also in last design, the diameter of hall in the anode is 15 mm and in tube (9) – 18 mm. For 1st version of Tomsk e-gun the insulator flange (1) with four electrical input (2) was constructed. For 2nd version the cathode support was reconstructed to provide quasi Piers surface, because it is used as the extractor electrode for e-beam.

Installation of Tomsk e-gun 1st version at ITEP e-MEVVA and experiments with it.

The Tomsk e-gun consists of the plasma generator, extraction system and e-beam transport channel with two coils (transport and focusing) and two plasma generators. The layout of Tomsk e-gun is shown in Fig.12. The length for e-beam transport channel from e-gun to MEVVA discharge was about 230 mm. As distinct from old e-MEVVA design, the strong axial magnetic field provides the transport of high current density e-beam along this channel. To install this e-gun at the ITEP e-MEVVA, the insulator flange with four electrical inputs has been constructed and manufactured. Two inputs provide electrical feed for the focusing coil, one for extracting electrode and one for plasma generators in transport channel. During our experiments, the plasma generators for compensation of e-beam space charge (pos. 8 in Fig.12) were not used. Their output was electrically connected with e-beam extractor electrode to MEVVA cathode. To provide the experimental works the following power supplies were constructed and manufactured:

- Power supply for anode coil of e-gun (PSAC)
- Power supply for transport coil (PSTC)
- Power supply for focusing coil (PSFC)
- Power supply (LC) for e-gun discharge

Electrical layouts of these power supplies are shown in Appendix.

In addition, the separate e-gun High Voltage platform (eHVp) for PSAC and LC has been constructed. To provide the timing of this power supplies, this platform has been provided by the fiber optic system.

For first experiments, the lead cathode with axial hole of 4 mm was used. The dimension of cathode has been taken from previous experience. However it was found that the hole has to be enlarged at least up to 11 mm. Such dimension has the melted spot on the surface of the MEVVA cathode support flange. See Fig.13. With hole of 4 mm it has been possible to operate with e-gun only without any magnetic field along e-beam. Under this condition, the density of e-beam at that flange has been low enough not to provide breakdown at the e-beam accelerating region. However the presence of magnetic field results in the increase of e-beam density and initiates the breakdown.

Taking into account this experimental fact, the new MEVVA cathode support flange for cathode with 12 mm hole has been constructed. Also several electrodes of MEVVA were modernized.

The best vacuum in experimental tank, which e-MEVVA is connected to, that could be obtained, when this version of e-gun has been installed, is $1*10^{-6}$ mBarr. The stable operation of the e-gun could be provided when vacuum in the experimental tank is better than $1.6*10^{-6}$ mBarr. The long drift tube (~600 mm) with small diameter (36 mm) reduces the vacuum condition and pumping possibility of the e-gun region. As a result, it was possible to provide the operation mode of e-gun (recommended by Tomsk) only for 2-3 hours. During this time the conditioning of the e-gun took at least one hour. The highest emission e-beam current was 10 A.

Disassembling of e-gun showed that e-beam still touches the MEVVA cathode support flange. The melting spot was moved a little (~1 mm) from axis (Fig.14). It is necessary to note that it moved exactly to the direction where the one of input wire for the focusing coil was located. It was observed twice with different alignment of focusing coil. It could be, that high current (100 A), flowing in this cable, interferences with e-beam along the short way, where they are parallel (1-2 mm), and bends it.

As it was written above, it was possible to provide stable operation of the e-MEVVA with the e-gun only for 2-3 hours. It is not enough for complete CSD measurement of ion beam generated by e-MEVVA with analyzing magnet. Nevertheless, it was possible to check the feature of separate peaks of interest. Such experiments have been done. It was found that amplitudes of following peaks – H^+, O^+, Pb^{2+}, Pb^{3+}, Pb^{4+} – didn't change their value for both mode (with/without e-beam). It was concluded that this version of e-gun didn't provide the e-beam with high enough density for increasing the charge states of ion beam generated by e-MEVVA ion source.

Installation of Tomsk e-gun 2nd version at ITEP e-MEVVA and experiments with it

The results obtained on Tomsk e-gun 1st version allow conclude that it is desirable to have MEVVA discharge aria as near as possible to e-beam extraction gap. For this goal, the Tomsk team sent us the new plasma flange for e-gun and we constructed the new insulator flange to adjust this new construction to our MEVVA part of e-MEVVA. The ITEP e-MEVVA with Tomsk e-gun 2nd t version is shown in Fig.15 and Fig.16. The electrical layout of ITEP e-MEVVA is shown in Fig.17. To feed the additional coil over the new insulator flange, the power supply for focusing coil can be used. The gap between the e-beam extracting electrode and MEVVA discharge atria in new assembling is 30 mm instead of 230 mm in Tomsk e-gun 1st version. The photo of experimental test-bench with new version of e-MEVVA is shown in Fig.18.

The new assembling immediately results improving of the vacuum. The vacuum of $5*10^{-7}$ mBarr in experimental tank has been obtained after two days of pumping. During experiments, the vacuum in experimental tank always was better than $8*10^{-7}$ mBarr. Also the conditioning of e-gun takes only a half of hour. As a result, the stable operation of e-gun can be supported for any desirable time. The maximum emission current of 25 A under 18 kV of e-beam accelerating voltage has been reached. The emission current is shown in Fig.19.

It is a place to note some difference of ITEP e-MEVVA from the HCEI Tomsk one. The main is a design of the plasma drift channel (PDC). The ITEP's one (pos. 8 Fig.15) mechanically and electrically separated from MEVVA anode (pos. 7) meanwhile in Tomsk version the MEVVA long anode used as PDC [4]. The metal pipe of PDC in ITEP e-MEVVA can be connected electrically to anode of MEVVA part, but for most experiments, it was fed by separate power supply. The total length of ITEP PDC is about 70 cm and diameter is 3.6 cm instead of 40 cm length and 4 cm diameter for the Tomsk's one. Therefore, to provide the same vacuum condition into e-gun region, more power pumping should be provided for ITEP e-MEVVA compare to Tomsk's one. From other hand, the longer PDC is used, the larger the time of interaction between plasma ions and e-beam. Therefore, to obtain the same $j\tau$ coefficient for increasing of ion charge states in ITEP e-MEVVA, the e-beam density can be smaller than in the Tomsk e-MEVVA.

The maximum emission current and the most stable operation condition has been obtained under following parameters of e-MEVVA.

- Discharge current at e-gun – 100 A
- Discharge current in MEVVA – 100 A
- Magnetic field in e-beam extraction gap – 0.5 kG
- Magnetic field in plasma drift channel – 0.5 kG

It is necessary to note that increasing of magnetic field either in plasma drift channel or in e-beam accelerating gap or in both coils together immediately brings to breakdown. It is necessary to note that such low magnetic field along ion source results low ion beam extracted from ion source. It provides some hardships for experiments that will be described below.

The accelerated e-beam has been detected at the output of ion source when the ion beam optic has been off. The Faraday cup is placed at the distance of about 1 meter besides the last grid electrode of ion beam optic. Nevertheless, the e-beam current of 20 mA has been detected. If the MEVVA discharge has been on, the e-beam current has been 120 mA (Fig.20). The several possible explanation of such e-beam current increasing at the FC can be suggested. First, the plasma of MEVVA discharge moves to the e-gun and provides the "flat" accelerating e-beam electrode, meanwhile without this plasma the e-beam extraction electrode has a large hole and a large radial component of extraction field. Second, the plasma of MEVVA works as the plasma lens for e-beam. Third, the plasma of MEVVA compensates the

charge of e-beam. It looks like all of them take place and improve transmission of e-beam throughout of ion source.

The ion beams without e-beam and with e-beam are shown in Fig.21. When the e-beam is on, it is easy to see influence of it on the ion beam. The ion beam has some valley during e-beam and an increase of amplitude after e-beam. Exactly this part of ion beam contains the ions with increased charge states.

The 2nd version of Tomsk e-gun provides the e-beam current density high enough to use it for experiments with e-MEVVA.

CSD measurements for Pb ion beam

The measured charge state distributions of lead ion beam generated by e-MEVVA with/without e-beam are shown in Fig.22. For "without e-beam" mode the maximum amplitude of signal was measured independently of it's time position along measured pulse. For "with e-beam" mode, the maximum amplitude of signal during and after e-beam injection time was measured only. Such method explains the large difference in amplitude of peaks corresponding to residual gas ions (like H^+, C^+, O^+). The main part of them is at the beginning of the ion current pulse and for "without e-beam" mode provides large amplitude of signal. The middle and end of beam pulse usually contain significantly less such kind of ions.

The one can see that e-beam significantly decreases the amplitude of Pb^{2+} peak (about five times). From other side, the e-beam increases the amplitude of Pb^{4+} peak. The amplitude of this peak increases about in one order. The peak of Pb^{3+} ions keep the same amplitude both for with e-beam and without e-beam mode. Therefore we can assert that e-beam increase the average charge of ion beam generated by ion source. It is impossible to say something definitive about generation of Pb^{5+} ions. As it was mentioned above, to transport e-beam to MEVVA and plasma drift tube region, we had to use the relatively low magnetic field along these regions. As result the generated ion beam has amplitude too low to provide measurements at the magnet analyzer. To increase the sensitivity of magnet analyzer, we had to reduce the resolution of measuring system. The identification of Pb^{2+} - Pb^{4+} ions did not make problem, but Pb^{5+} ions peak could not be separated from next ones. Also small sensitivity of MA explains the absence of charge-exchange peaks in CSD. Such kind of peaks usually has amplitude one order less than the "original" ones.

The presence of Fe^+ and Zn^+ ions in CSD for "with e-beam" mode indicates that e-beam touches somewhere the surface of ion source.

Conclusion

For e-MEVVA ion source, in frame of the contract, the e-guns with different kind of cathodes (fiber, "semiconductor" and "ceramic") were investigated. It was found that for every type of the cathodes the electrons are extracted from boundary of plasma generated in e-gun. The e-gun with "ceramic" cathode was chosen for all experiments with e-beam thanks the best stability of e-beam parameters and the longest lifetime.

The experiments with basic version of e-MEVVA with "short" e-beam (when length of e-beam pulse is shorter than the length of discharge pulse) and "long" e-beam (when length of e-beam pulse is longer than the length of discharge pulse) were carried on. On the base of these experiments it was concluded that it is necessary to design the new version of MEVVA generator for e-MEVVA. This design has to provide the length of e-beam drift space between e-gun and plasma aria as short as possible. Such new MEVVA plasma generator was designed and manufactured. Also the new magnetic coils for plasma drift channel and e-beam drift channel were constructed and installed at the new version of e-MEVVA ion source.

The new e-MEVVA ion source were investigated with two version of Tomsk e-gun, designed and manufactured specially for these experiments. The main result of these experiments is a conformation of the e-MEVVA idea. The 20 kV e-beam with beam current of 25 A increases the mean charge state of lead ion beam. The e-beam significantly decreases the amplitude of Pb^{2+} peak (about five times). From other side, the e-beam increases the amplitude of Pb^{4+} peak. The amplitude of this peak increases about in one order. The peak of Pb^{3+} ions keeps the same amplitude both for with e-beam and without e-beam mode.

The obtained results stimulate us to plan the further investigations on optimization both e-MEVVA design and its' parameters for advance the e-MEVVA concept to increase the charge states of heavy ion beams. Particularly it is interesting for beam of uranium ions.

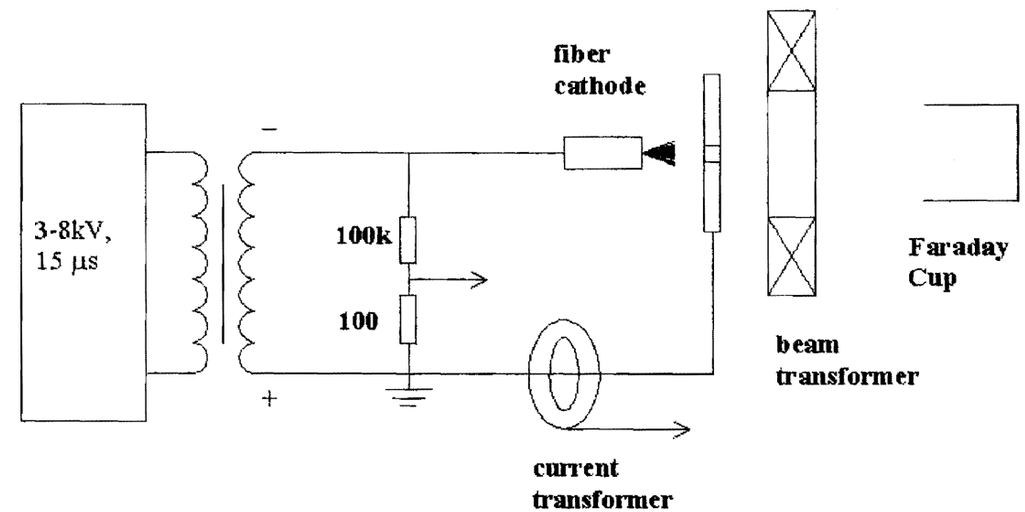

Fig. 1. Layout of power supply and measurement equipments for e-gun with fiber cathode

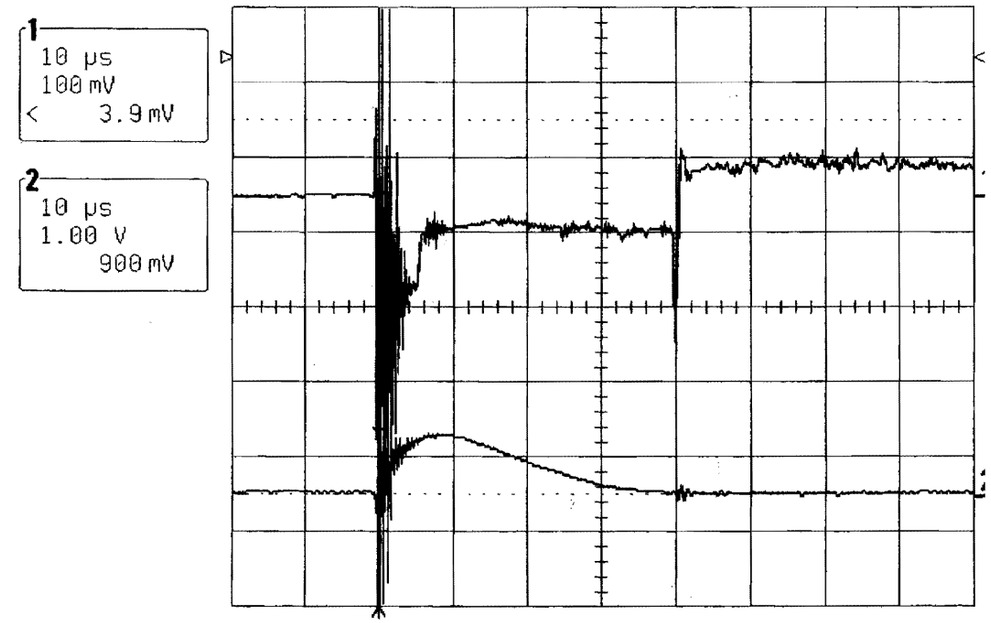

Fig. 2. 1 - Anode-cathode voltage drop (100 V/dev) and 2 - discharge current (440 A/dev) for e-gun with fiber cathode

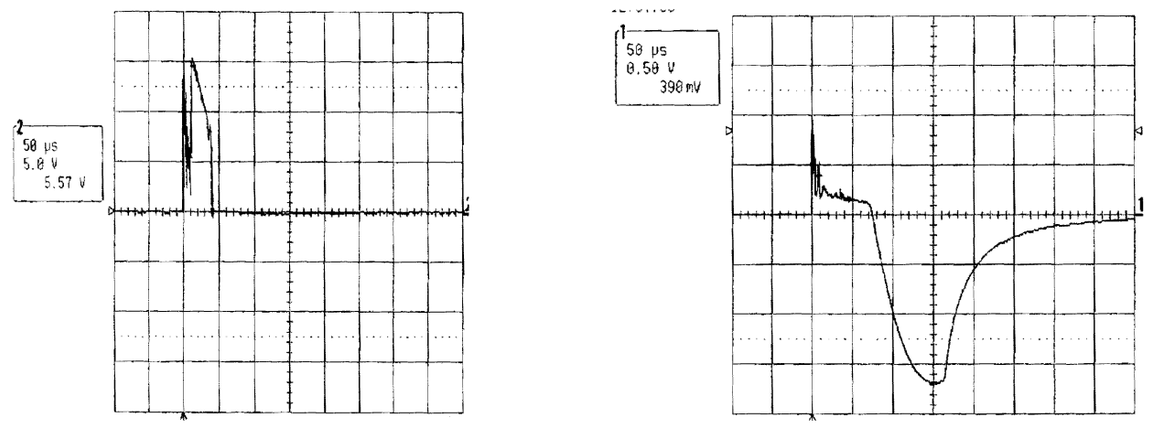

Fig. 3. 1 - Anode-cathode voltage drop (500 V/dev) and 2 - discharge current (500 mA/dev) for e-gun with fiber cathode

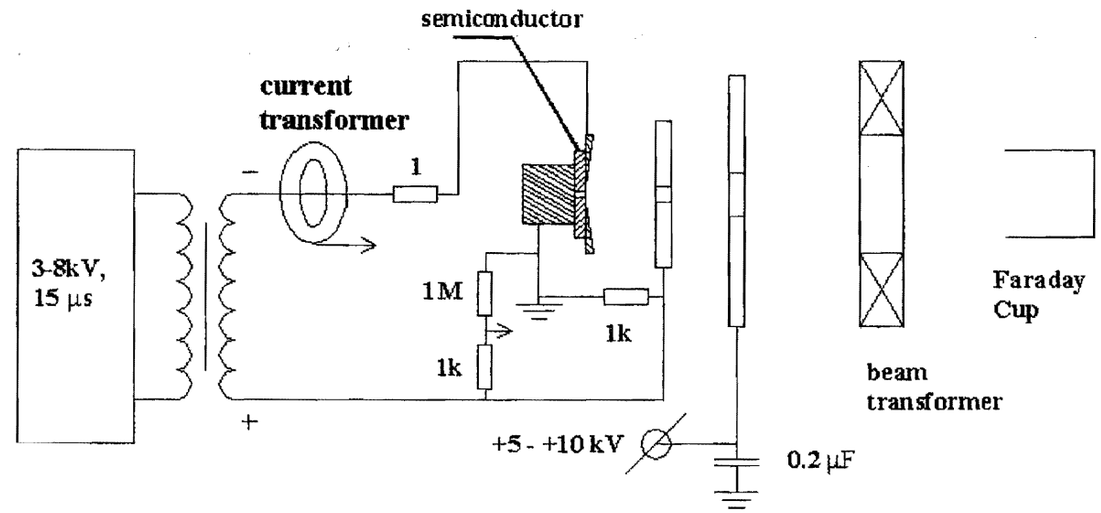

Fig.4. Layout of power supply and measurement equipments for e-gun with semiconductor cathode

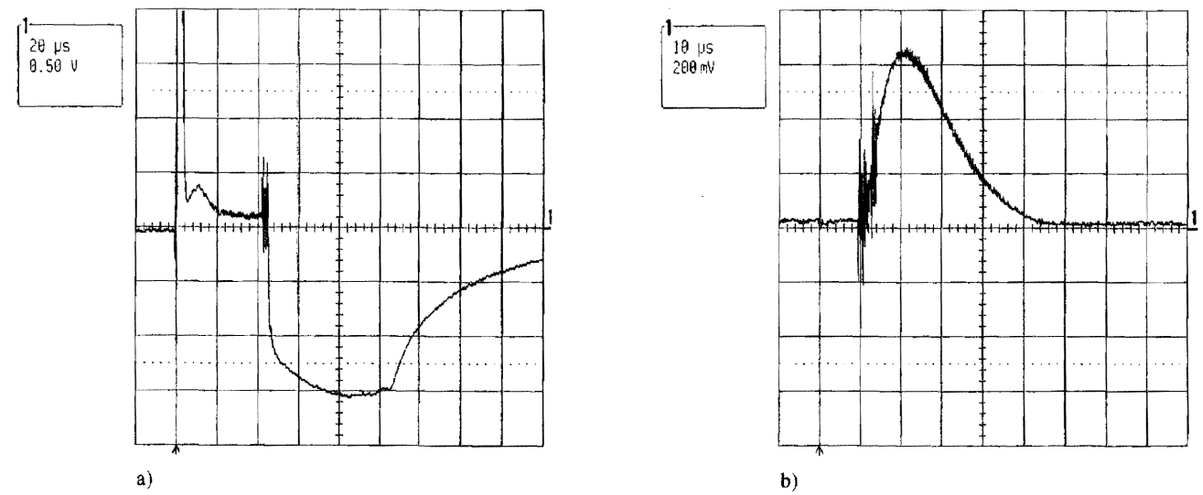

a) b)

Fig. 5. a) Anode-cathode voltage drop (50V/dev) and b) current in cathode circuit (170A/dev) for e-gun with semiconductor cathode

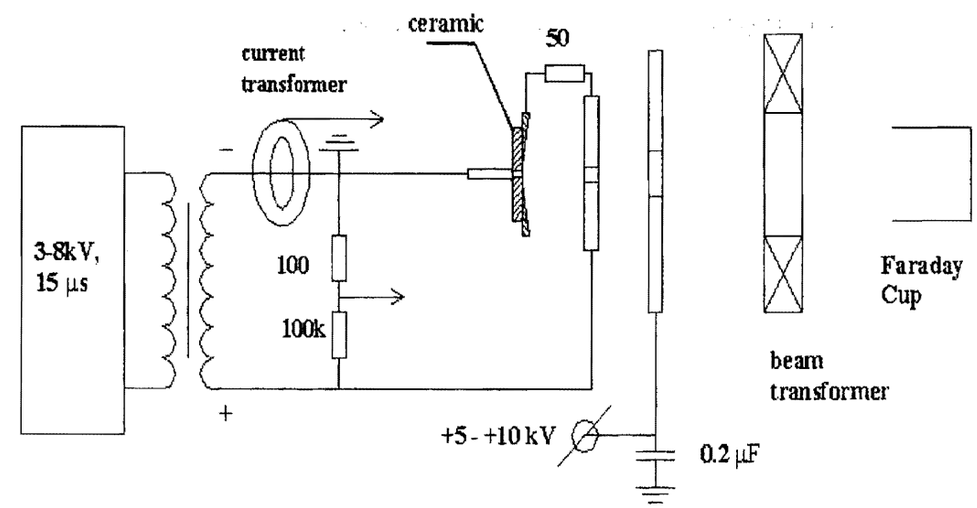

Fig. 6. Layout of power supply and measurement equipments for e-gun with ceramic cathode

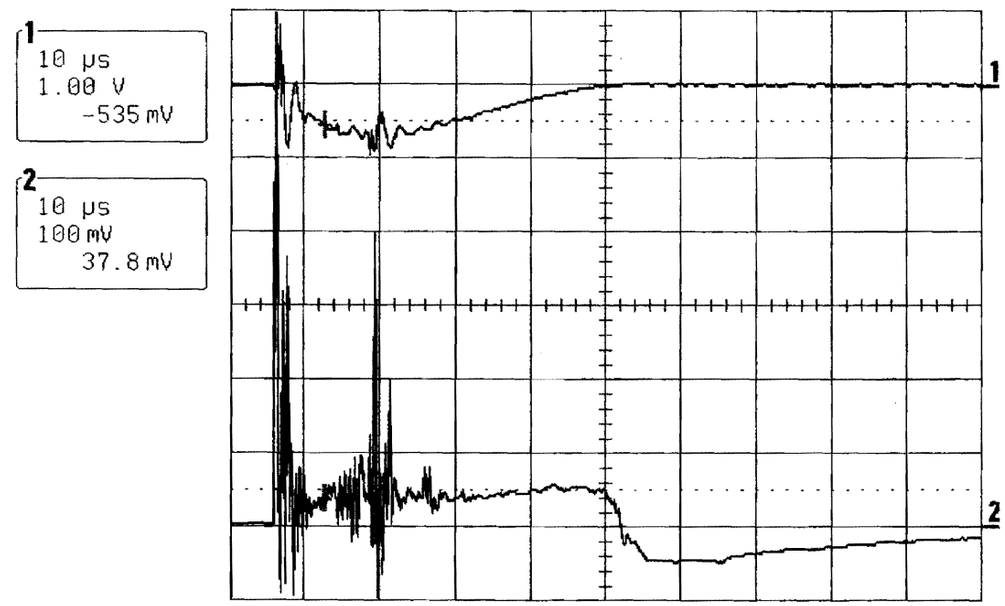

Fig.7 1) Current in cathode circuit (440 A/div) and 2) voltage drop (100 v/div) for e-gun with ceramic cathode

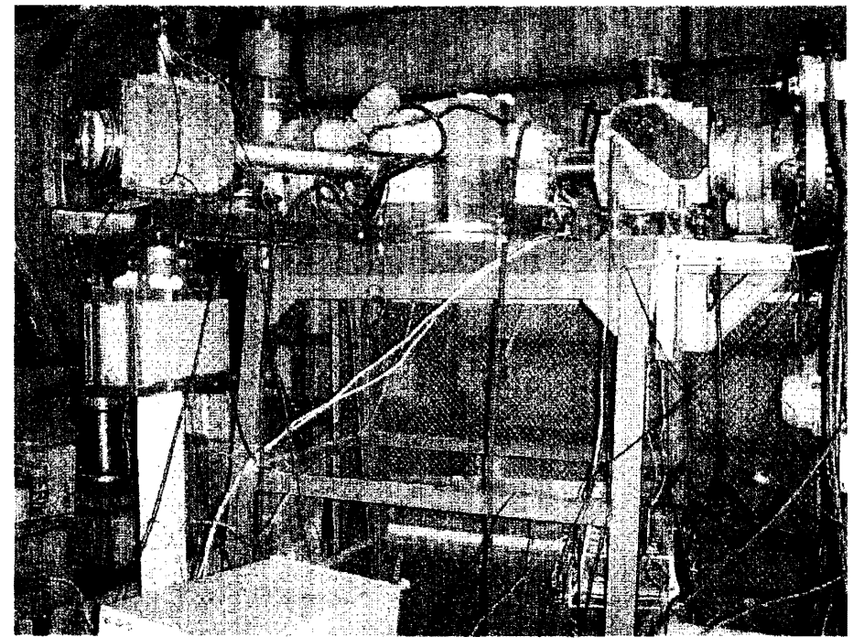

Fig. 8. Photo of magnet analyzer.

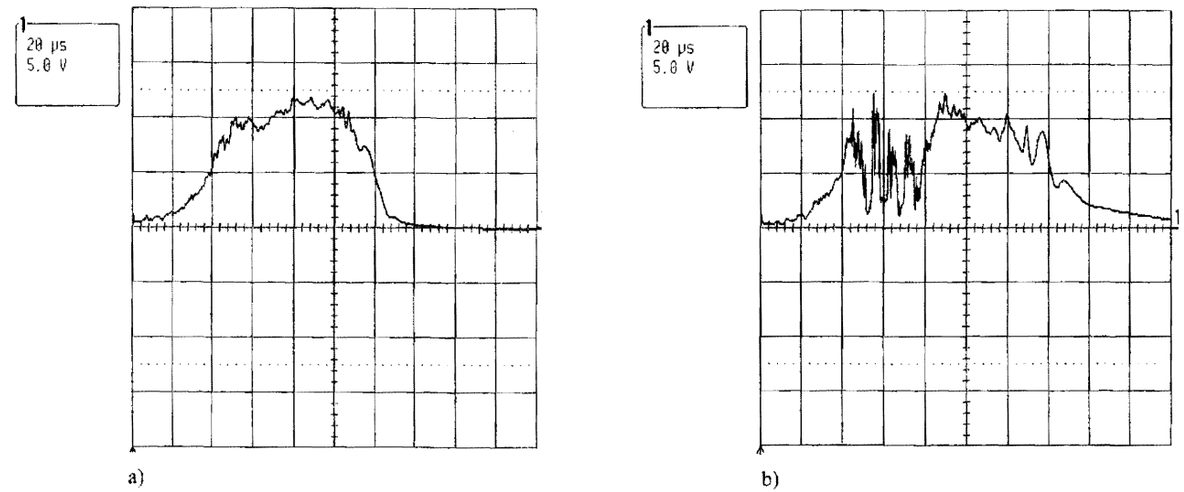

Fig. 9. Ion beam pulse from e-MEVVA (a) without and (b) with e-beam. Basic version of e-MEVVA

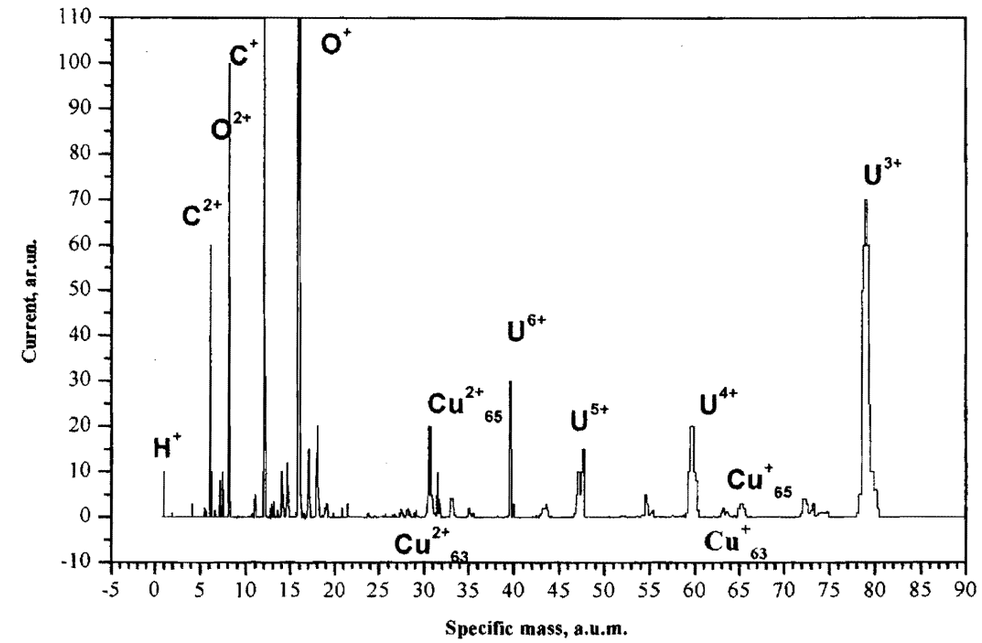

Fig. 10a. CSD of uranium beam from e-MEVVA with e-beam and before it

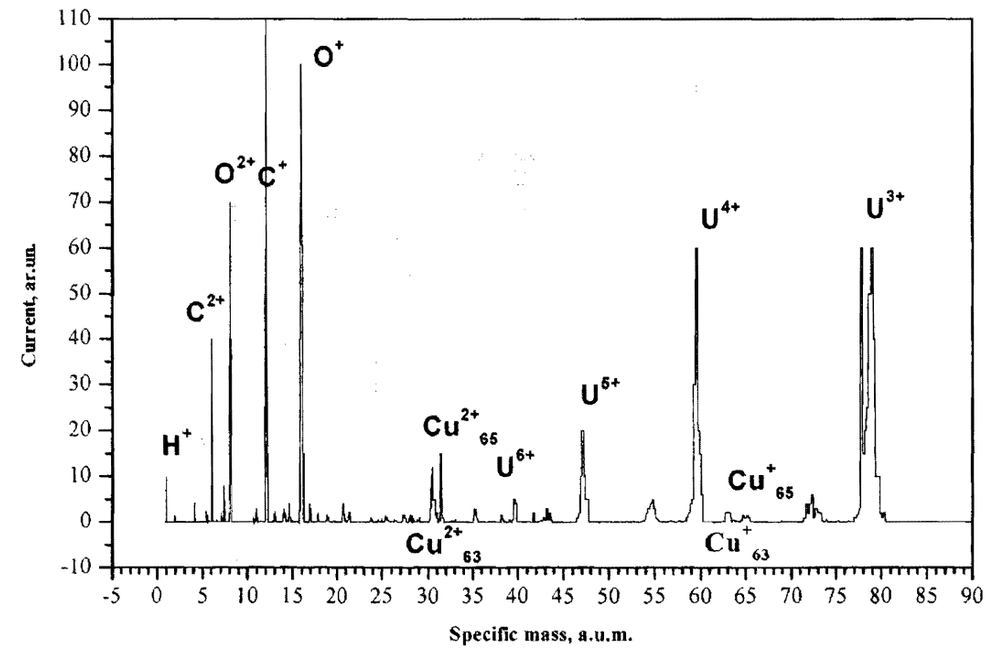

Fig. 10b, CSD of uranium beam from e-MEVVA with e-beam and after it

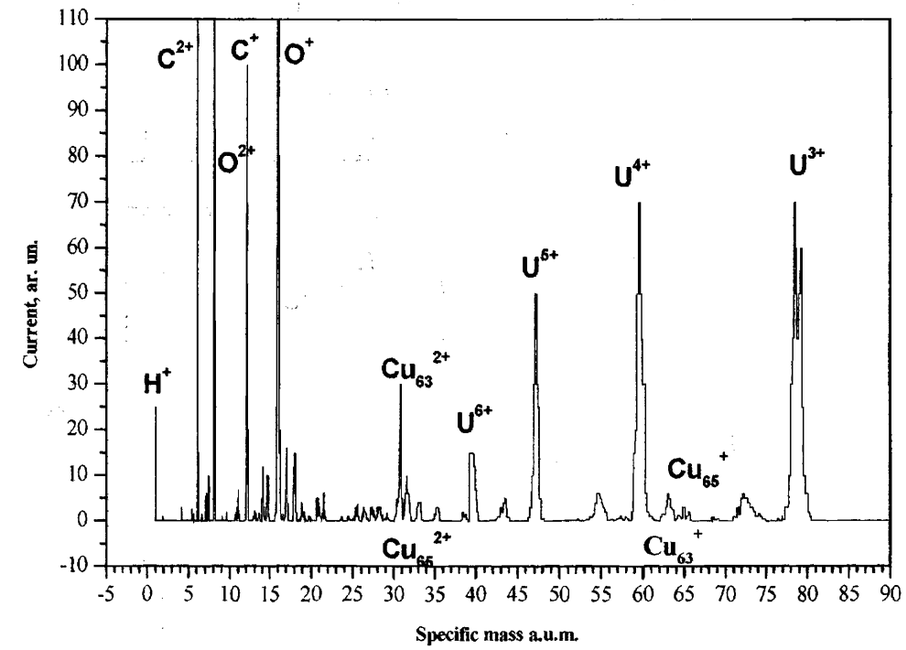

Fig. 10c, CSD of uranium beam from e-MEVVA without e-beam

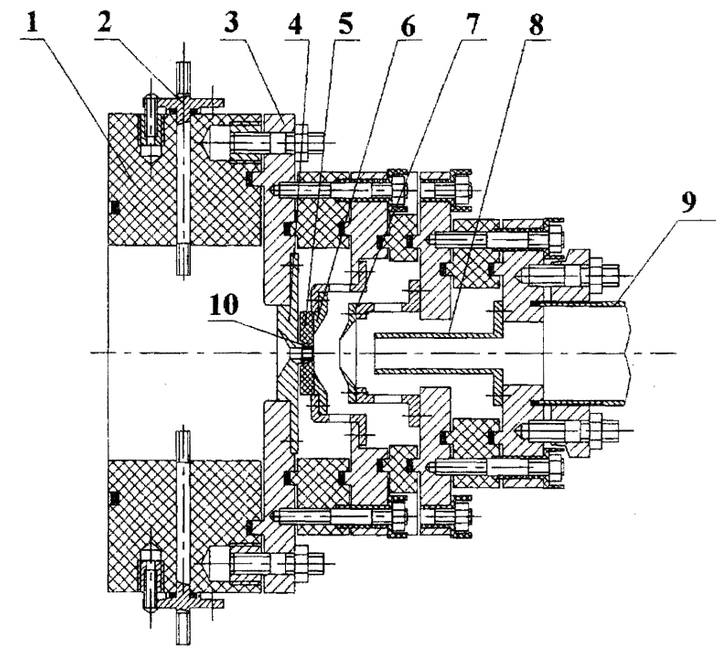

Fig. 11. Design of new MEVVA plasma generator for e-MEVVA ion source.

1 – Adjusting insulator flange, 2 – electrical input, 3 – cathode flange, 4 – cathode support, 5 – ceramic insulator, 6 – trigger, 7 – anode, 8 – tube enlarging PDC, 9 – PDC, 10 – cathode.

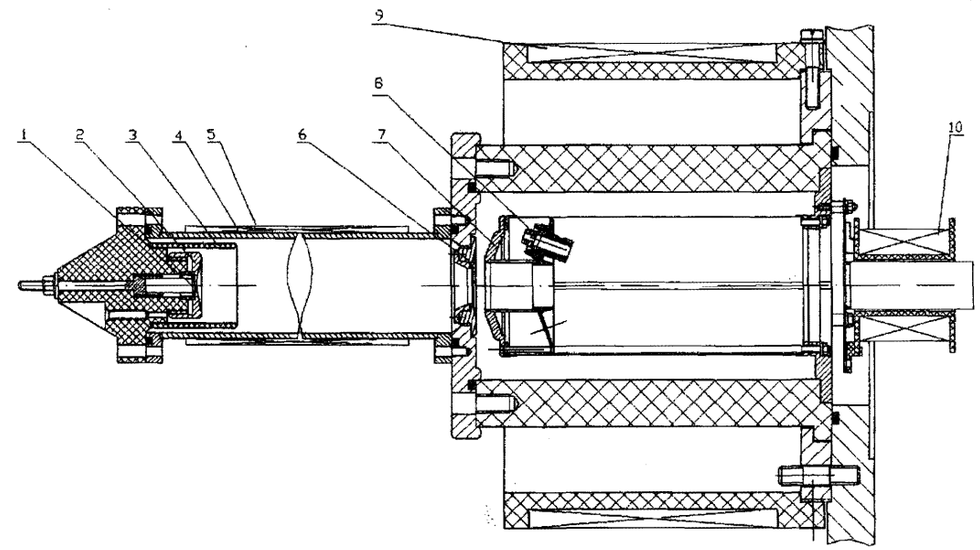

Fig. 12. First version of Tomsk e-gun (with long e-beam transport channel).

1 – cathode, 2 – trigger, 3,4 – anode, 5 – anode coil, 6 – plasma grid electrode, 7 – e-beam accelerating electrode, 8 – plasma generator, 9 – transport coil, 10 – focusing coil.

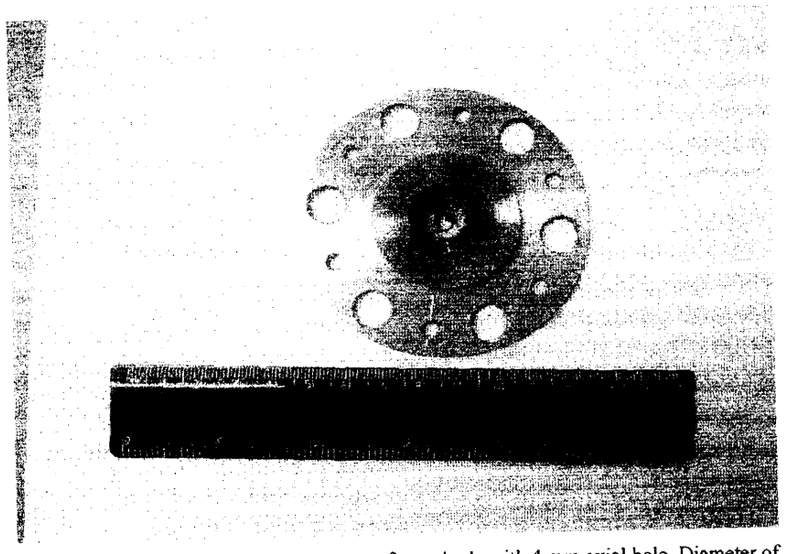

Fig. 13. Photo of MEVVA cathode support for cathode with 4 mm axial hole. Diameter of melting spot – 11 mm.

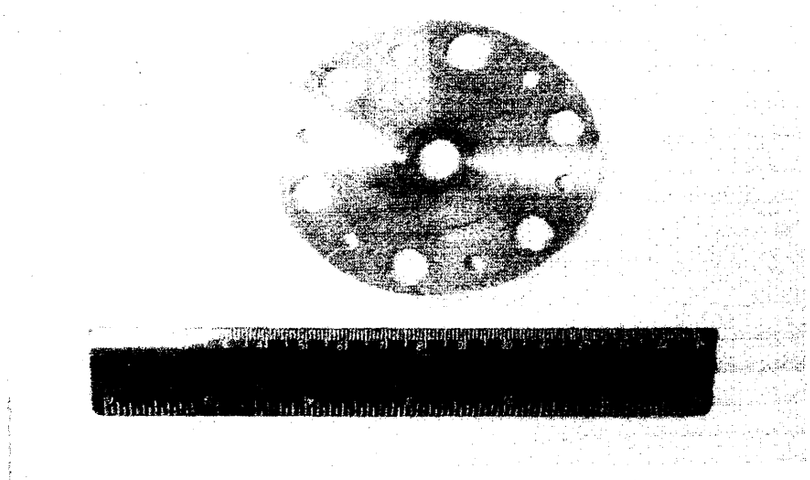

Fig. 14. Photo of MEVVA cathode support for cathode with 12 mm axial hole.

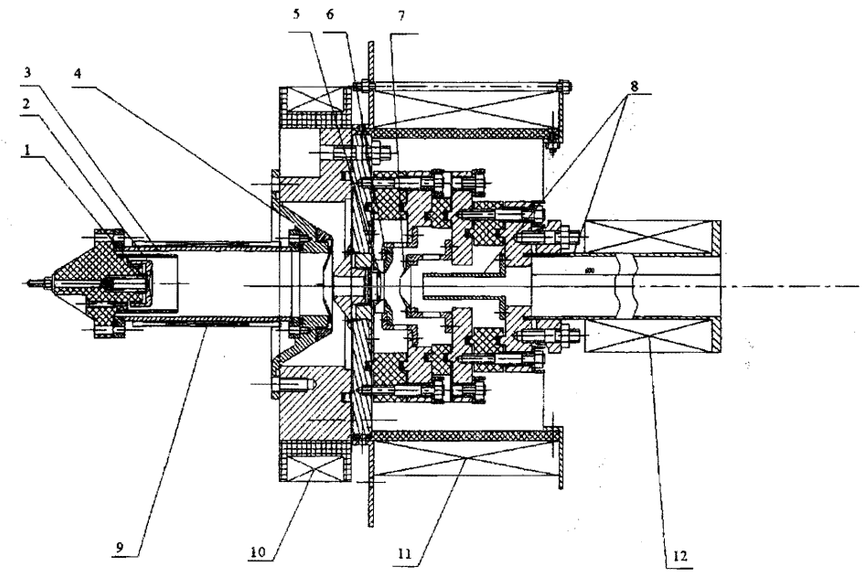

Fig. 15. ITEP e-MEVVA with Tomsk e-gun.

1 – e-gun cathode, 2 – e-gun trigger, 3 – e-gun anode, 4 – e-beam extracting electrode, 5 – MEVVA cathode, 6 – MEVVA trigger, 7 – MEVVA anode, 8 – Plasma Drift Channel, 9 – e-gun anode coil, 10 – transport coil, 11 – MEVVA coil, 12 – PDC coil.

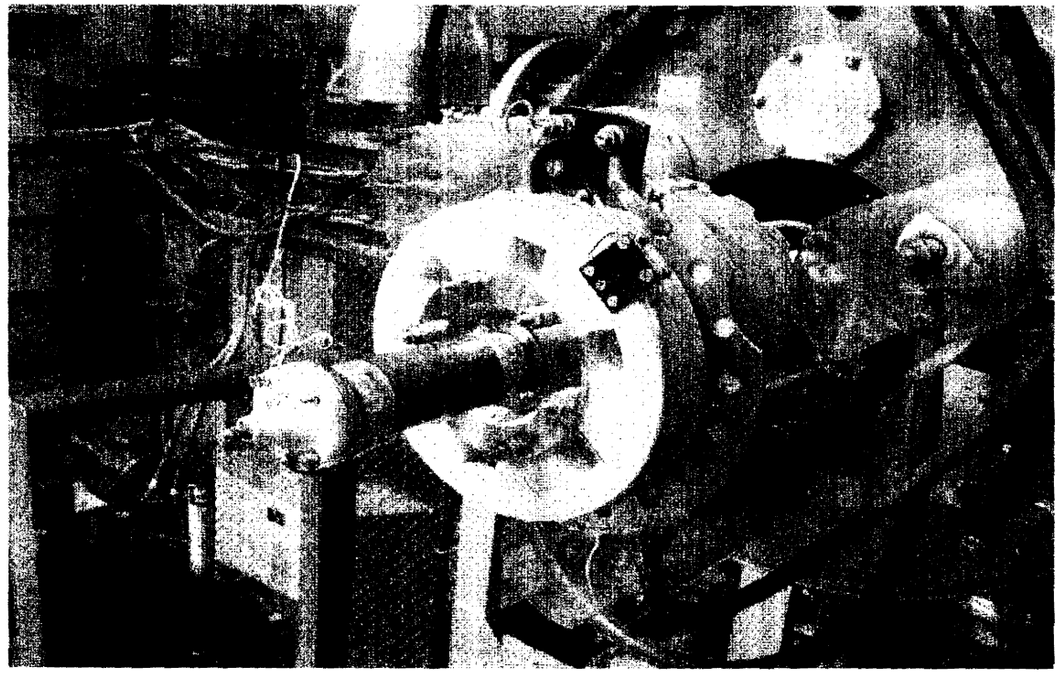

Fig. 16. Photo of e-MEVVA with Tomsk e-gun 2nd version.

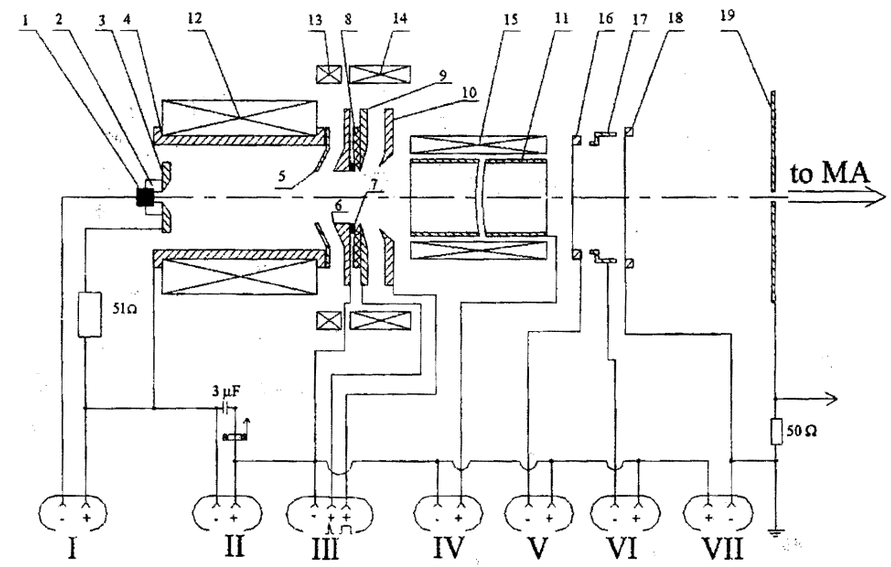

Fig. 17. ITEP e-MEVVA with Tomsk e-gun.

1 – e-gun cathode, 2 – e-gun insulator, 3 – e-gun trigger, 4 – e-gun anode, 5 – e-gun plasma grid, 6 – e-beam extracting electrode, 7 MEVVA cathode, 8 – MEVVA insulator, 9 – MEVVA trigger, 10 MEVVA anode, 11 – plasma drift channel, 12 – e-gan anode coil, 13 – transport coil, 14 – MEVVA coil, 15 – PDC coil, 16 – ion beam extractor, 17 – focusing electrode, 18 – ground electrode, 19 – first slit at the input of MA.

I – Trigger pulse for e-gun, II – accelerating e-beam voltage, III – MEVVA discharge pulse voltages, IV – potential at the PDC, V – ion extraction voltage, VI – ion beam focusing voltage,

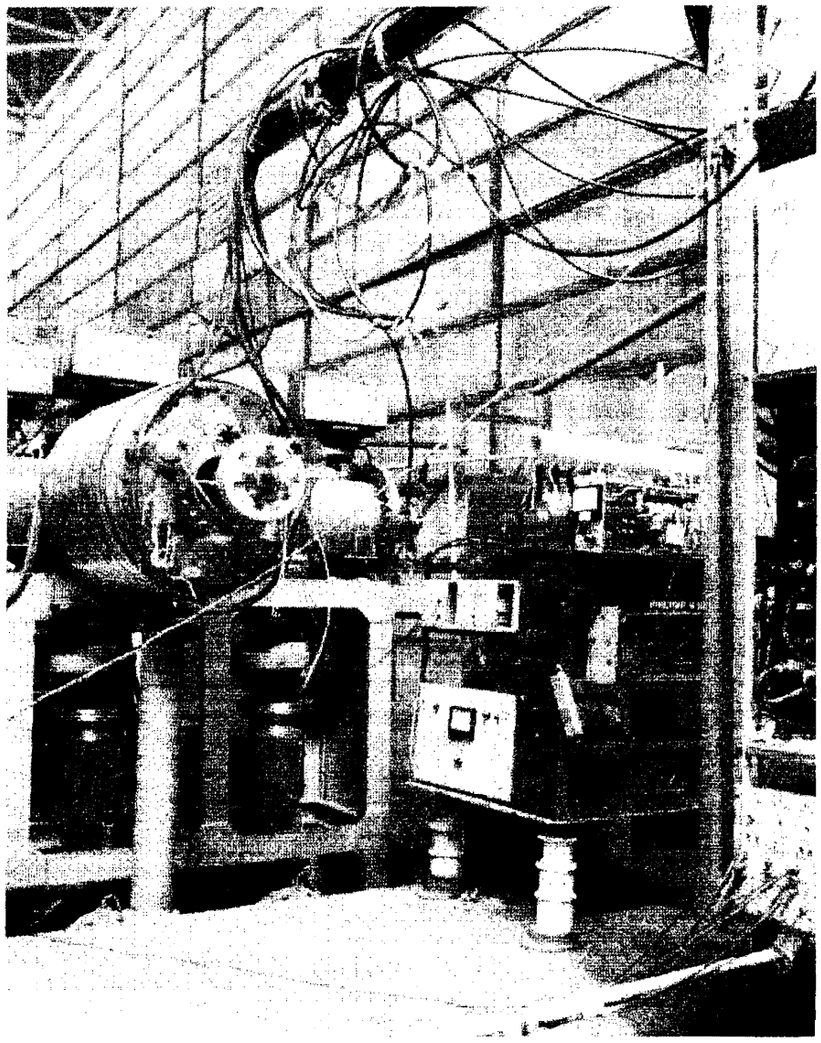

Fig. 18. Photo of experimental test-bench with new version of e-MEVVA and 2nd version of Tomsk e-gun..

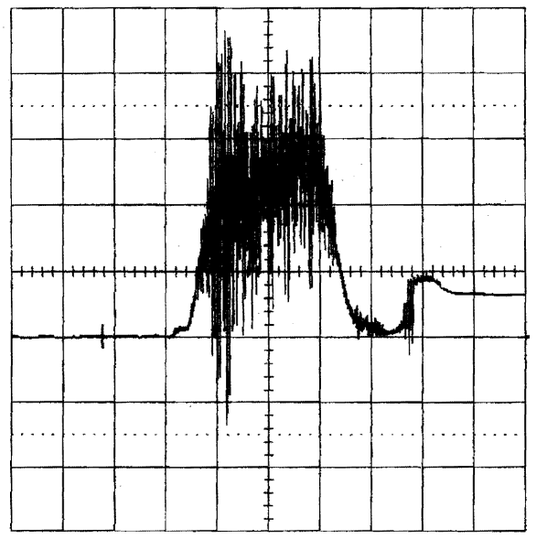

Fig. 19. E-beam emission current, 10A/dev, 20 μs.

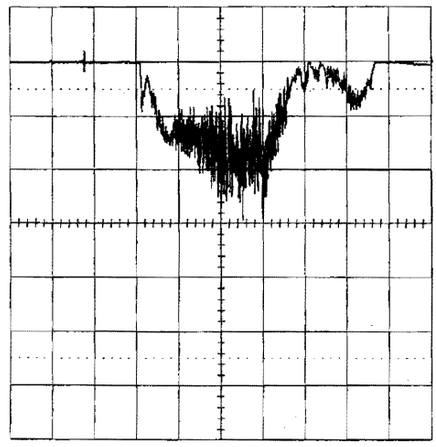

Fig. 20. a) E-beam current at the ions source output (MEVVA off), 10 mA/dev, 20μs/dev.
New version of e-MEVVA with Tomsk e-gun 2nd version.

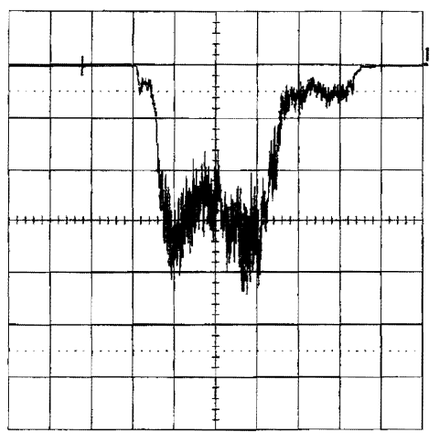

Fig. 20. b) E-beam current at the ions source output (MEVVA on), 40 mA/dev, 20μs/dev.
New version of e-MEVVA with Tomsk e-gun 2nd version.

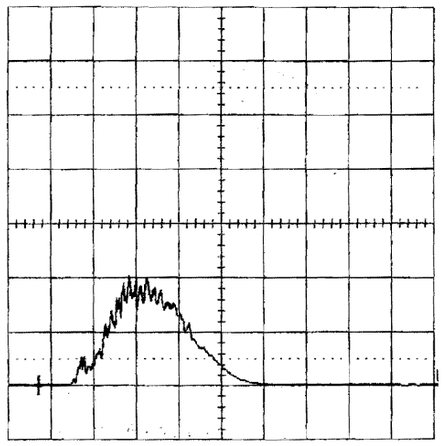

Fig. 21. a) Ion beam at the output of e-MEVVA without e-beam. 10 mA/dev. 50 μs/dev.
New version of e-MEVVA with Tomsk e-gun 2nd version.

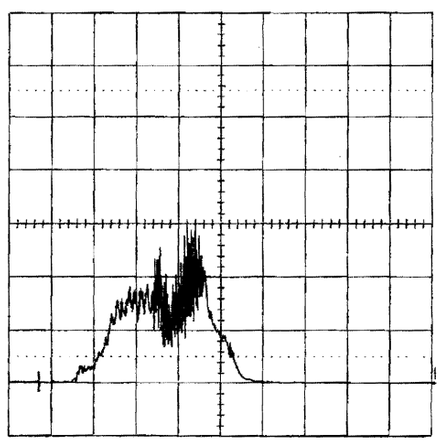

Fig. 21. b) Ion beam at the output of e-MEVVA with e-beam. 10 mA/dev. 50 μs/dev.
New version of e-MEVVA with Tomsk e-gun 2nd version.

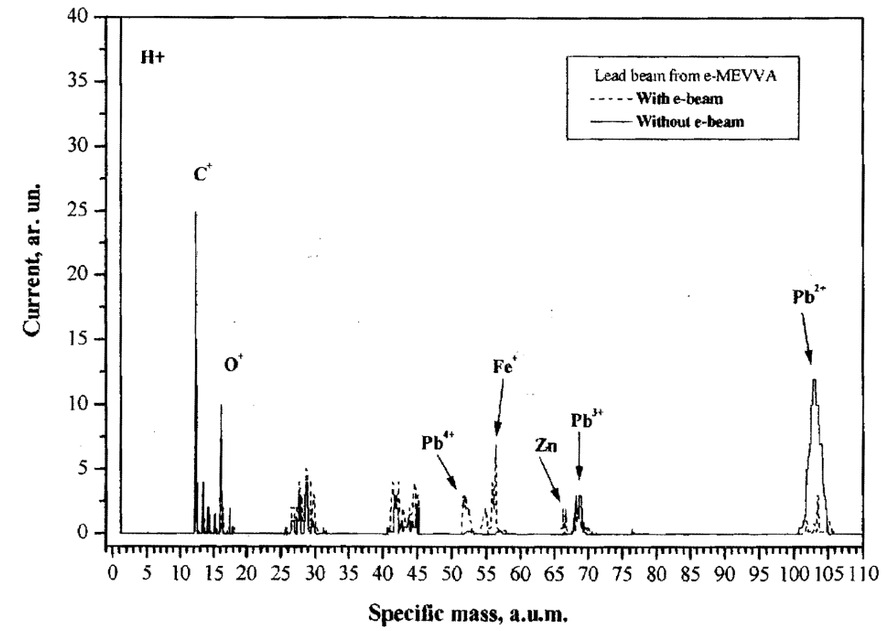

Fig. 22. Spectrum of Pb ions beam from ITEP e-MEVVA with (black) and without (red) e-beam

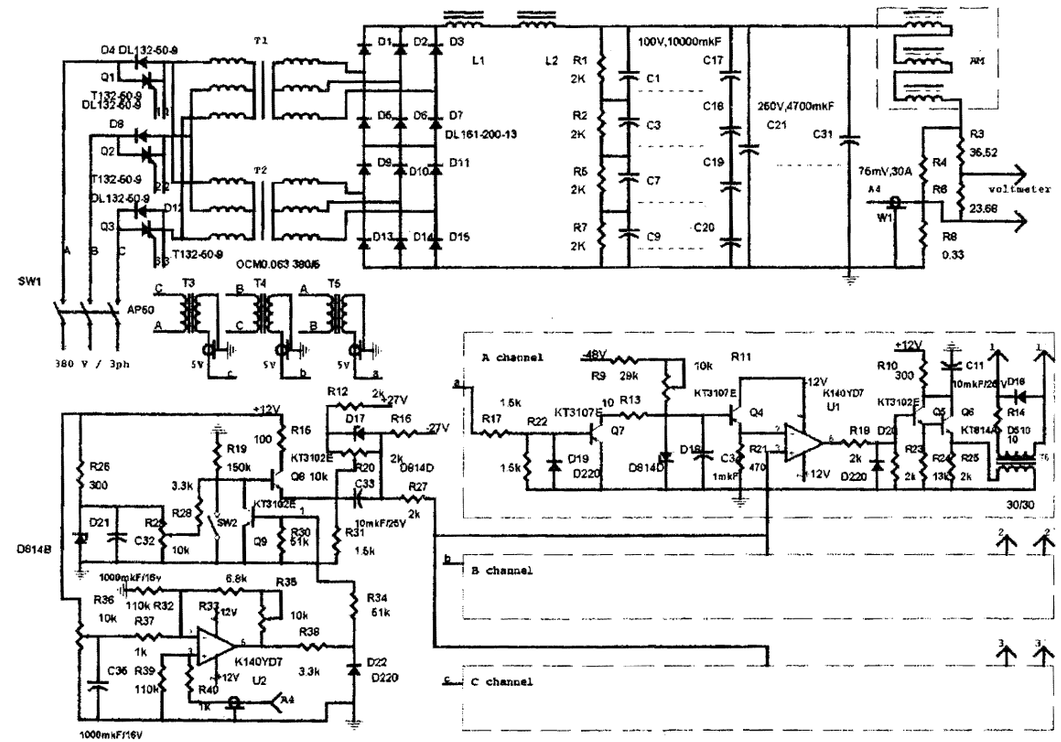

Fig. 23 The analyzing magnet power system scheme.

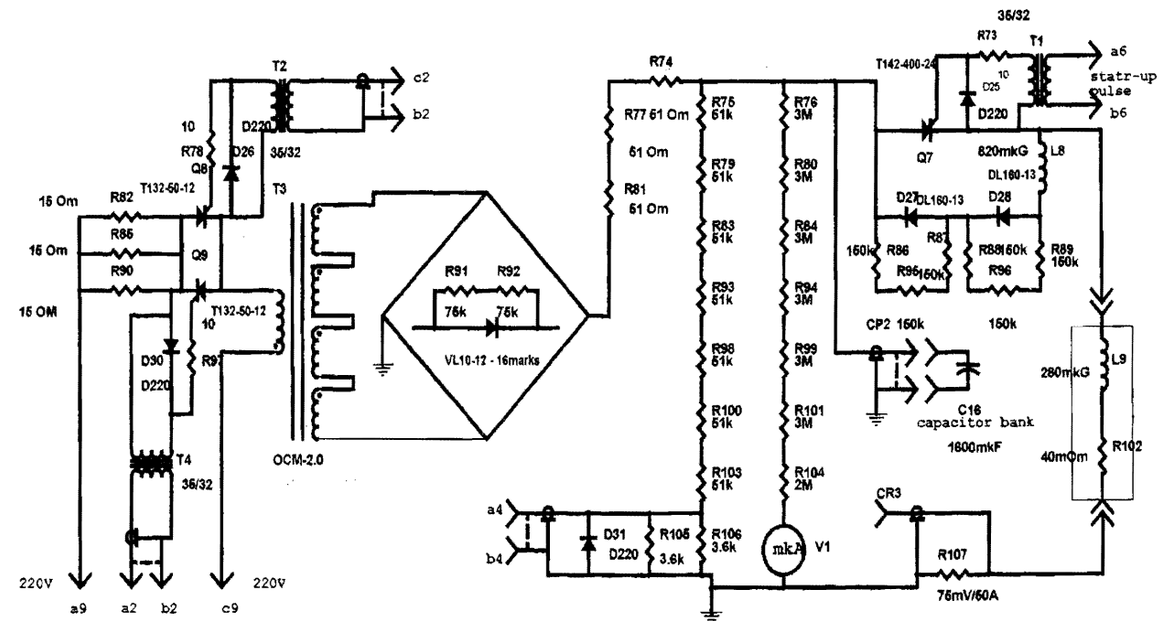

Fig. 24 The block scheme of power supply for PDC coil

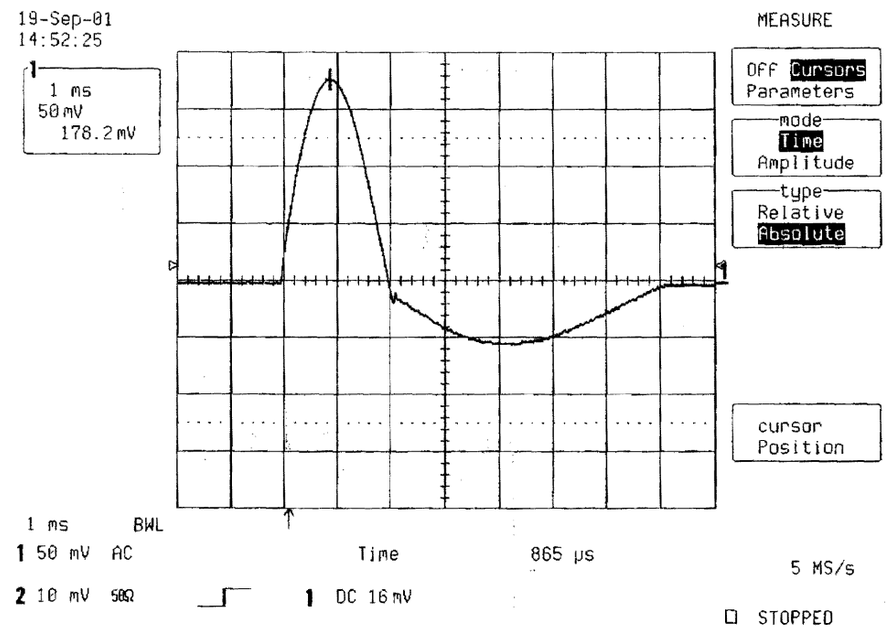

Fig. 25 The current waveform in the PDC coil

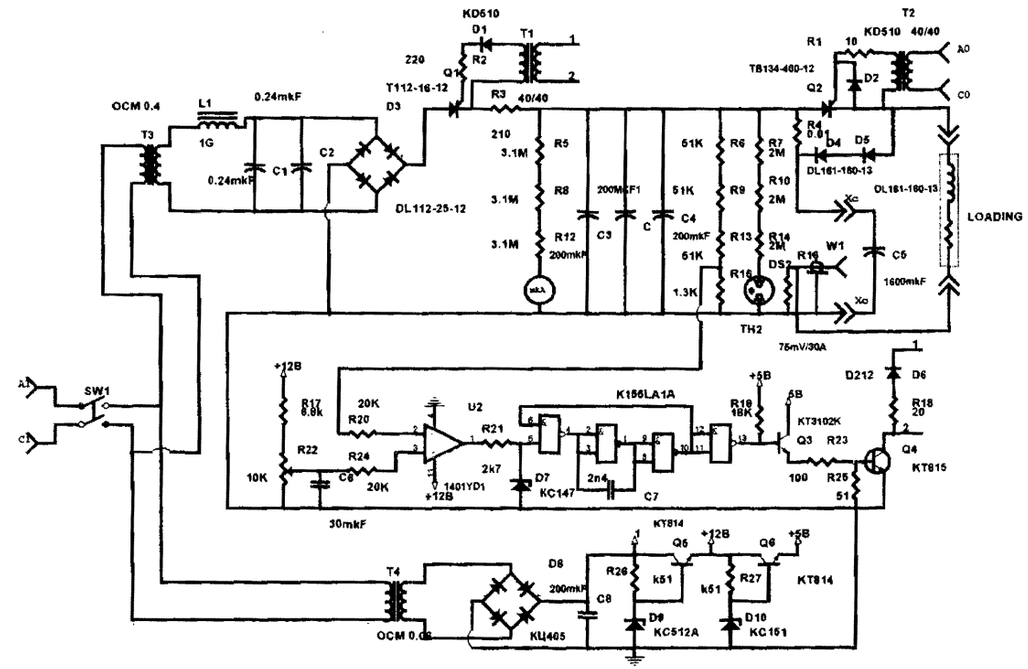

Fig. 26 The block scheme of power supply for MEVVA coil

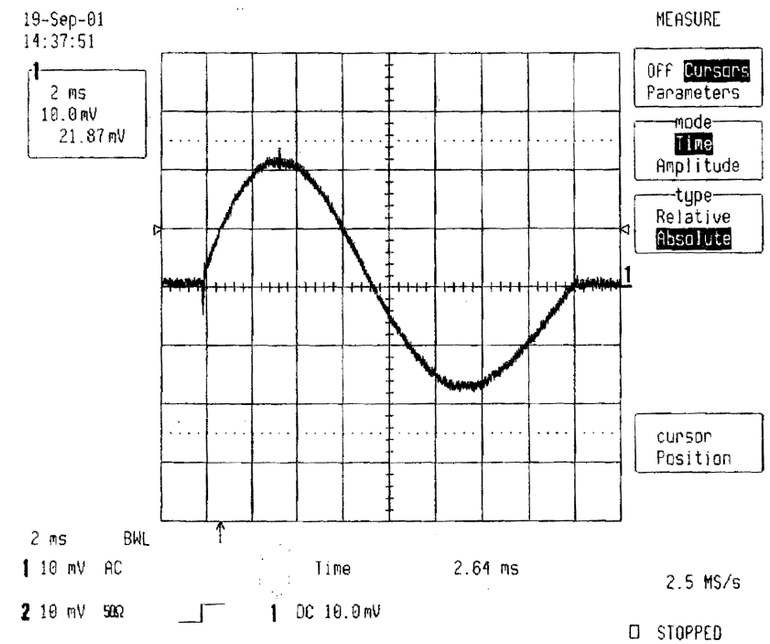

Fig. 27 The current waveform in the MEVVA coil

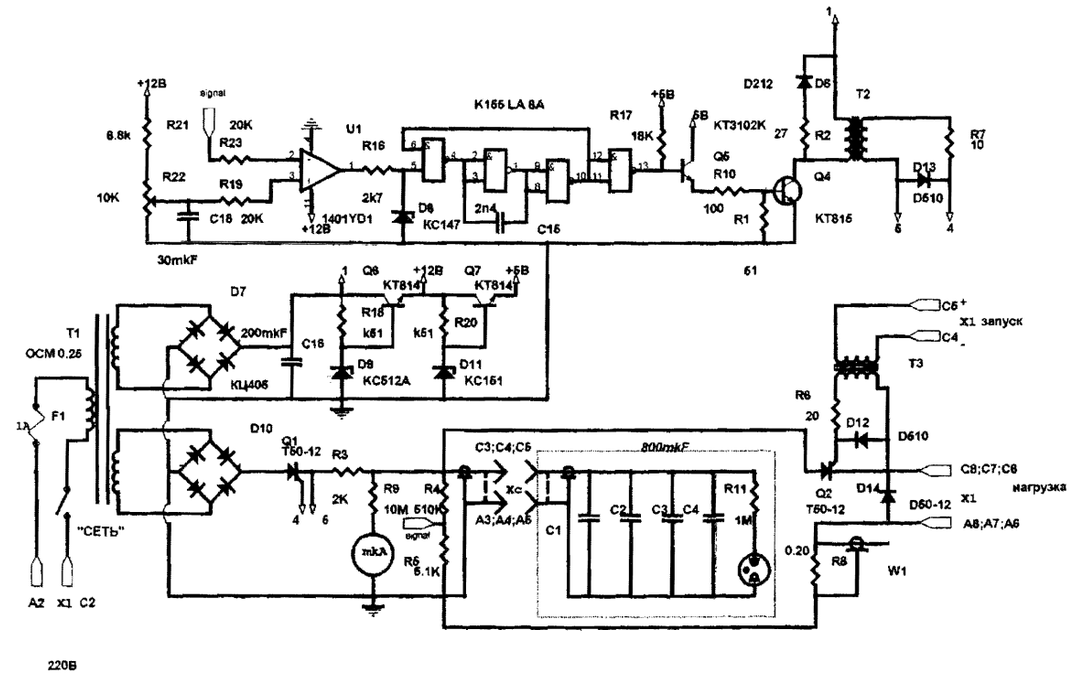

Fig. 28 The block scheme of power system for the e-gun anode magnet

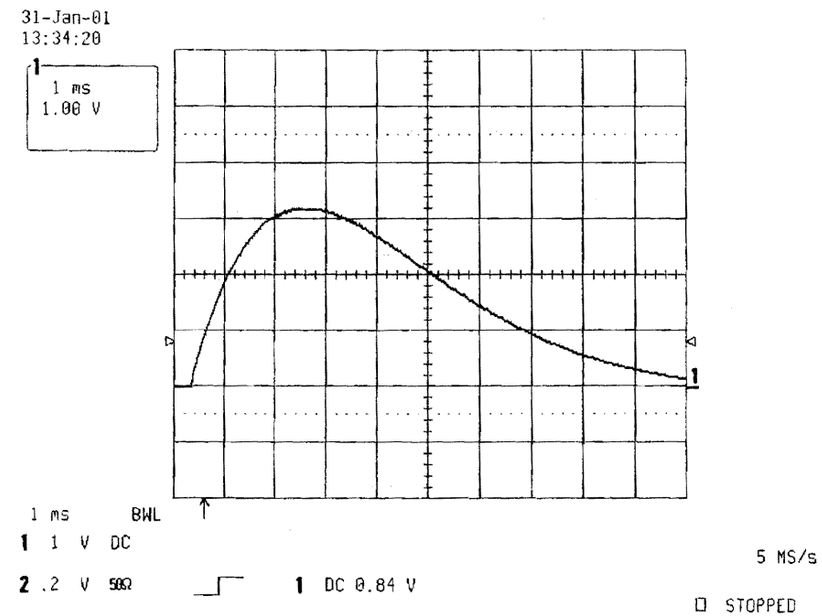

Fig. 29 The current waveform in the e-gun anode magnet

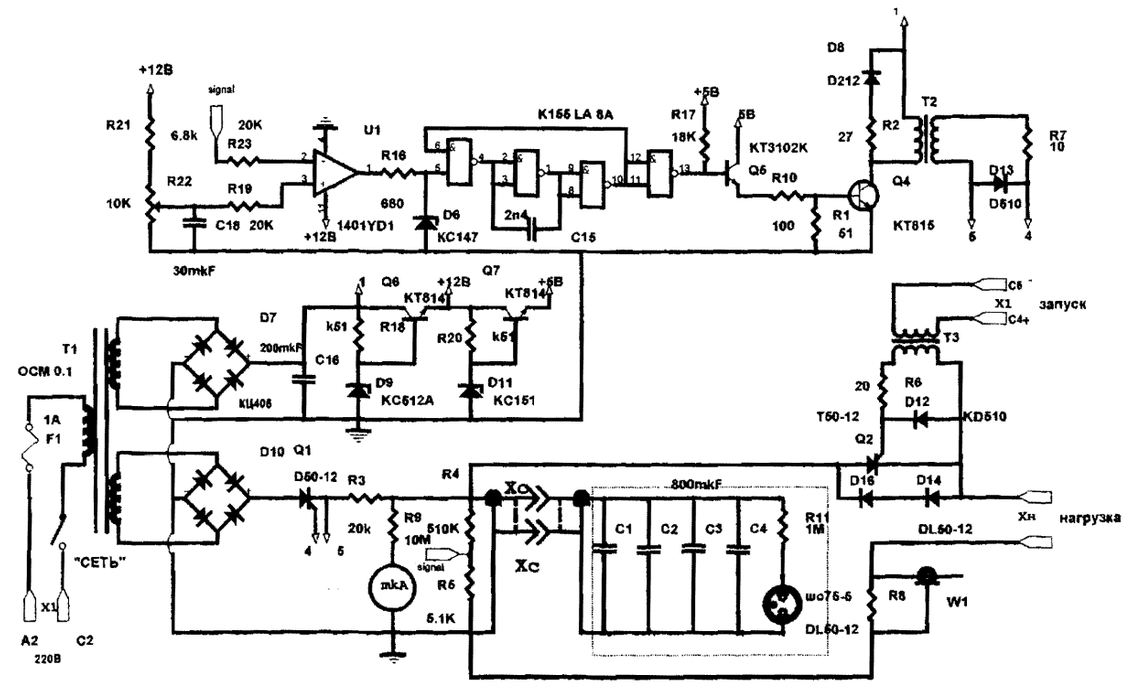

Fig. 30 The block scheme of power supply for e-beam transport coil

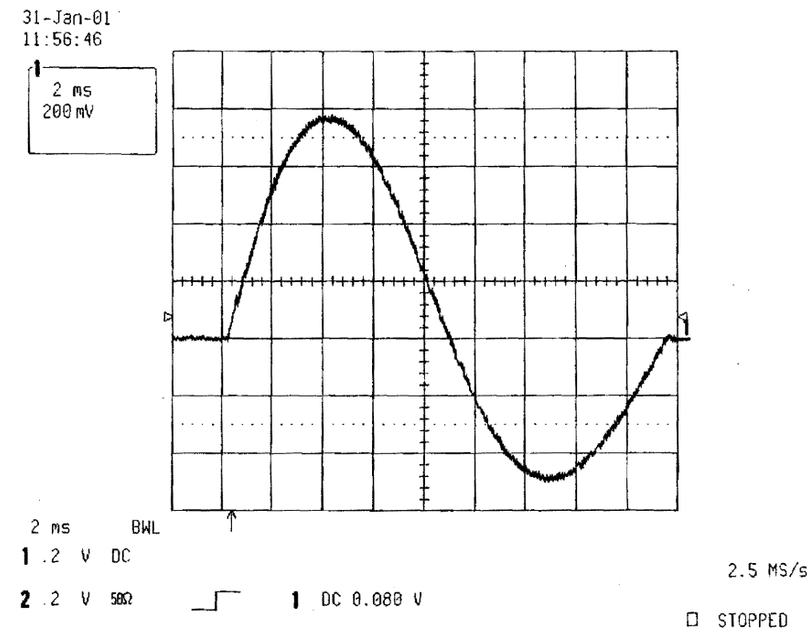

Fig. 31 The current waveform in e-beam transport coil

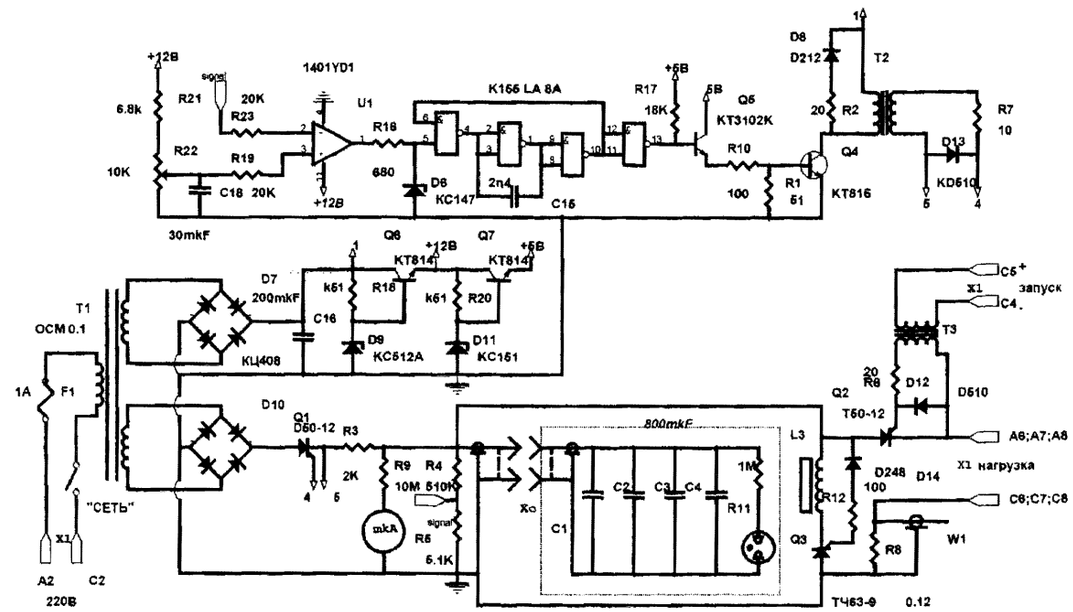

Fig. 32 The block scheme of power supply for the e-beam focusing coil.

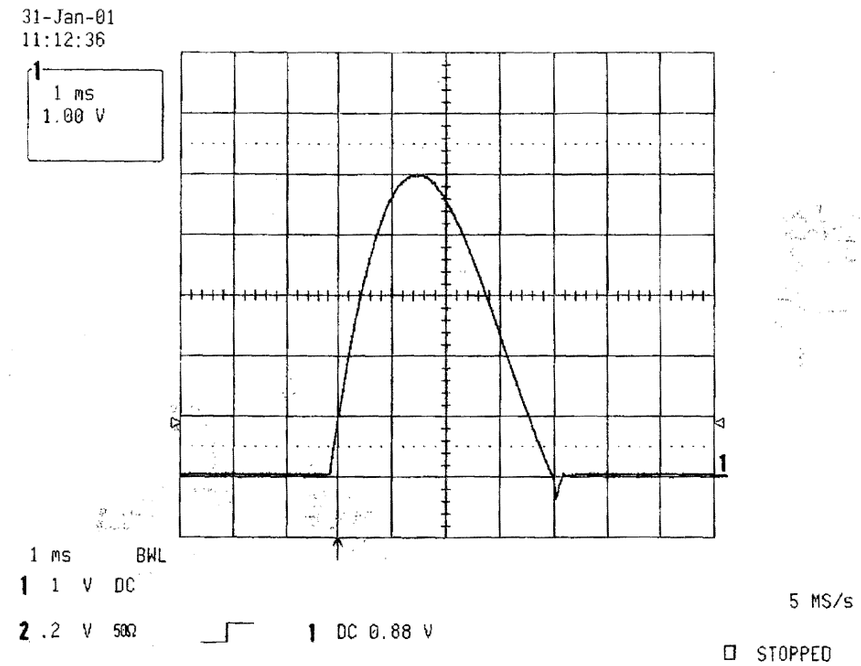

Fig. 33 The current waveform in for the e-beam focusing coil.

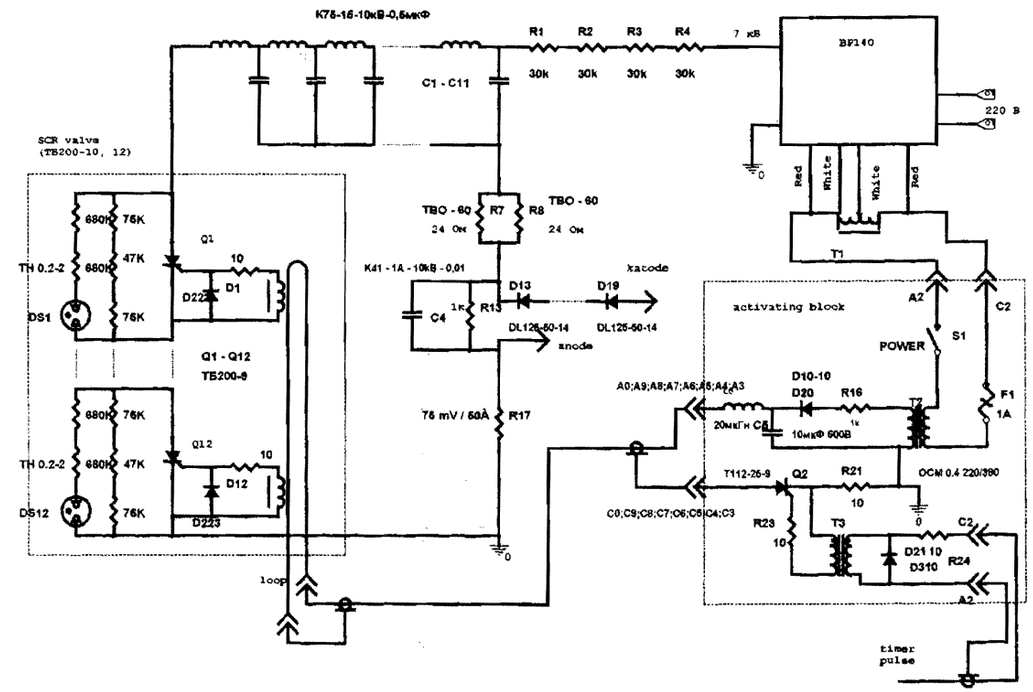

Fig. 34 **The block scheme of power system for the electron plasma emitter discharge (EPED).**

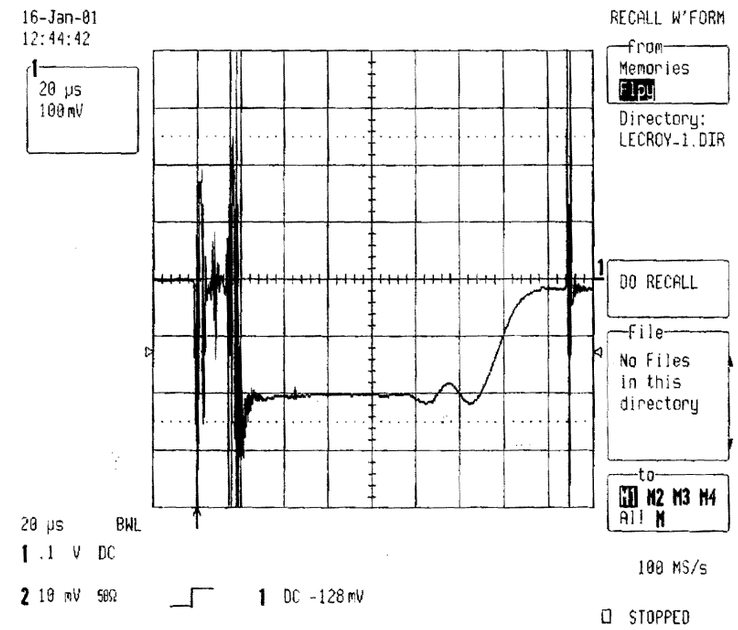

Fig. 35 The current waveform from power supply for EPED in the real load at 6 kV in the capacitors. The flat pulse peak current is 213 A. The pulse duration (on the base) is 130 µc

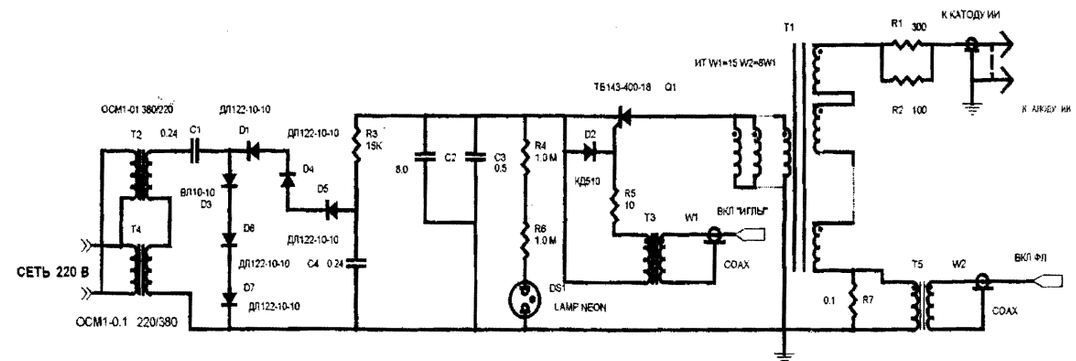

Fig. 36 The block scheme of power system for shot pulse generator

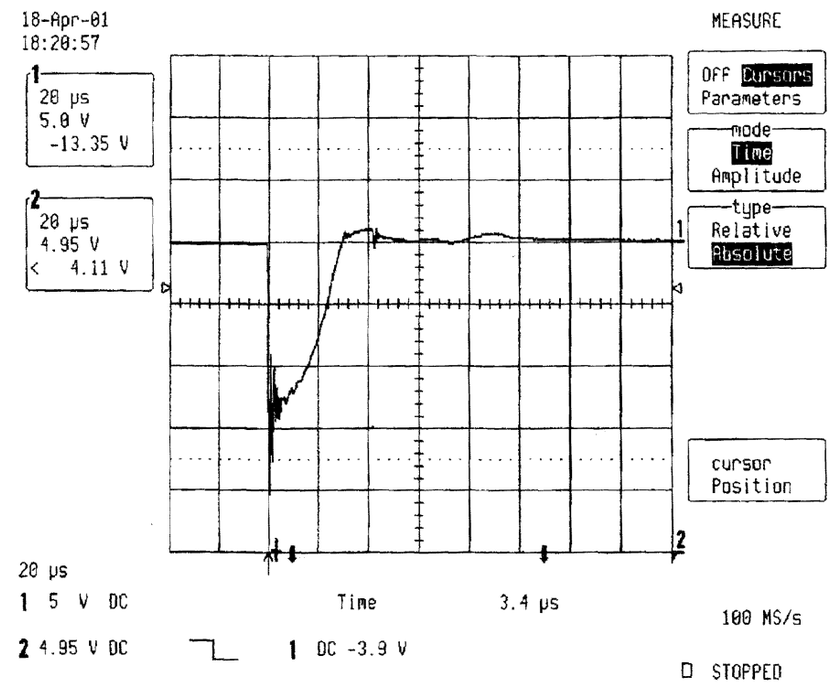

Fig. 37 The high voltage pulse waveform from power system for shot pulse generator

Reference

[1] G. Brown. Rev. Sci. Instrum., **65**, 3061 (1994).
[2] H. Reich, P. Spadtke and E.M. Oks Rev. Sci. Instrum. **71**, 707 (2000).
[3] N.V Gavrilov and E.M Oks. Nucl. Instrum. and Meth. in Phys. Res. **A 439**, 31 (2000).
[4] E.M. Oks, I.G. Brown, M.R. Dickinson, R.A. MacGill, P. Spadtke, H. Emig and B.H.Wolf., Appl. Phys. Letters. July, 10, 200 (1995).
[5] E.M. Oks, A. Anders, I.G. Brown, M.R. Dickinson and R.A. MacGill. IEEE Trans. on Plasma Science. **24**, 1174 (1996).
[6] A.S Bugaev, E.M Oks, G.Yu Yushkov, A. Anders and I.G. Brown. Rev. Sci. Instrum. **71,** 701 (2000).
[7] A. Anders, G. Yu. Yushkov, E.M. Oks, A.G. Nikolaev and I.G. Brown. Rev. Sci. Instrum. **69,** 1332 (1998).
[8] E. Donets. Rev. Sci. Instrum. **69,** 614 (1998).
[9] V.A. Batalin, Yr.N. Volkov, T.V. Kulevoy, S.V. Peternko// Proc.Intr.Conf. Linac-94, 1994, Tsukuba, Japan, p.390-392;
V.A. Batalin, Yr.N. Volkov, T.V. Kulevoy, S.V. Peternko// Proc.Intr.Conf. EPAC-94, 1994, London, England, p. 1560-1562.
[10] A. Hershcovitch, B.M. Jonson, F. Liu, A. Anders and I.G. Brown. Rev. Sci. Instrum. **69,** 798 (1998).
[11] Field emission cathodes using commercial carbon fiber, R. Prohaska and A. Fisher, Rev. Sci. Inst., 53(7), 1982, pp.1092-1093.
[12] The special modification of the MEVVA ion source (e-MEVVA) with the external electron beam and the drift channel for high charged ions generation, V.A. Batalin, Yr.N. Volkov, T.V. Kulevoy, S.V. Petrenko.
[13] Ion Charge State Distribution in High Current Vacuum Arc Plasmas in a Magnetic Field, E.M. Oks, A. Anders, I.G. Brown, M.R. Dickinson, R.A. MacGill, IEEE, V.24, N.3, June 1996, pp.1174-1183.
[14] Alexey Bugaev et al., "Electron-Beam Enhancement of Ion Charge State Fractions in the Metal-Vapor Vacuum-Arc Ion Source", Applied Physics Letters, to be published.

Appendix

Layouts for power supplies constructed for support experiments with e-MEVVA during 2000 – 2001

The analyzing magnet power system

The principled scheme of analyzing magnet (AM) power system is shown in Fig.23. The magnet is the load of the powerful 3-phase controlled rectifier, which consists of the T1, T2 transformers and 2 diode bridges connected in series. The pulsations of the rectifier output are limited by the LC filter (L1, L2, C1, C31). The regulation of the magnet current is carried out by the phase control of the supply line voltage at the rectifier output. The thyristor-diode modules are tapped in series with each pair of the same-phase supply line windings of the T1, T2 transformers. Each of these thyristors is initiated by the palces formed in one of the 3 identifical A, B,C channels of the control scheme. Each channel consists (A for example) of a T5 phase transformer, notched voltage generator, a pulse with modulation modulator, a Q6 power amplifier and an output isolated T6 pulse transformer. The R36 resistor controls the phase angle of thyristor "turn on" state. The voltage tapped off the R36 resistor is used to control the stage assembled at the U2 opamp.

The voltage from the water-cooling oil shunt proportional to the magnet current is applied to the other amplified input. The operation amplifier output signal controls the work of the amplifying stage, utilizes the Q8, Q9 transistors. The signal from the output of the amplifying stage is applied to the pulse with modulation modulator of the thyristor channels start-up.

The current in the winding of the AM can change is value from 1.5 to 22A.The minimum current step is 4mA.The pulsation rate in the upper level of the magnet current range isn't in excess of 0.02%.

The maximum dissipation power in the magnet winding 3kW.

Power supply for PDC coil

The power system consists of 3 separate blocks: a power block, a control block and a block with the capacitor bank. The total capacity of the capacitor bank is 1200mkF (100mkF/2000V, 12). It is not necessary to take into consideration the power polarity of the capacitor bank. The coil consists of 190 turns and its inductance is 280 μG.

The power block scheme is shown in Fig.24. The regulation of the voltage in capacitor bank is carried out by the phase control of the supply line voltage at the rectifier output. The thyristor module is tapped in series with the primary winding of the T3 power transformer. According to the scheme the C16 capacitor bank take a charge through the Q8, Q9 thyristors, T3 power transformer and the R74, R77, R81,

R82, R85, R90 limited resistors. The capacitor bank discharge takes place through the Q7 thyristor activated by the timer signal.

The D27, D28 diodes are designed for preservation of energy accumulated in the coil.

The current waveform in the transport coil is shown in Fig.25. The waveform is tapped from the R107 viewing current resistor (75mB/50A) at 300 V (30marks) in the capacitor bank. Attenuator reduces the signal in 10 steps.

Each of these thyristors is initiated by the pulses formed in one of the 2 similar A, B channels of the control scheme (Fig3). Each channel (for example A channel) consists of a T5 phase winding of T4 transformer (Fig.4), notched voltage generator, a U6 pulse with modulation modulator, a Q3 power amplifier and an output isolated T2 pulse transformer.

Digital to analog converter (SW1, SW2, SW3, U1, U3, U4, U5) controls the phase angle of thyristor "turn on" state. The voltage tapped off the converter is used to control the stage assembled at the U2 opamp.

The voltage from the R104, R106 resistors of measuring divider is proportional to the capacitor banc voltage is applied to the other amplified input.

The operation amplifier output signal controls the work of the amplifying stage, utilizes the Q5, Q6 transistors.

The signal from the output of the amplifying stage is applied to the pulse with modulation modulator of the thyristor channels start-up.

The current in the winding of the coil can change its value from 100 to 3800A. The minimum current step is 4A.

Power supply for MEVVA coil

The power system consists of 2 separate blocks: a power block and a block with the capacitor bank. The total capacity of the capacitor bank is 1600mkF (200mkF/1000V, 4). It is not necessary to take into consideration the power polarity of the capacitor banc. The coil consists of 115 turns and its inductance is 2.2 mG.

The power block scheme is shown in Fig.26. According to the scheme the C2-C4 power block capacitors and capacitor bank take a charge through the Q1 thyristor and the R3 limited resistor till the voltage tapped off from the R8 divider resistor isn't on target with the voltage specified by the R22 resistor. At this moment the signal on Q1 thyristor control electrode equals to zero and the thyristor goes to the OFF state. The capacitors discharge takes place through the Q2 thyristor activated by the timer signal.

The D4, D5 diodes are designed for preservation of energy accumulated in the coil.

The current waveform in the transport coil is shown in Fig.27. The waveform is tapped from the R16 viewing current resistor (75mB/30A) at 290 V (29marks) in the capacitor banc. Attenuator reduces the signal in 10 steps.

The R22 capacitor voltage control handle, the load current control connector (W1), the capacitor voltage indicator are on the front panel of the block .The 220 V power and the timer's cable are joined up with X1 connector. The capacitor bank is joined up with the Xc connector. The load is joined up with the XL connector. The X1, Xc, XL connectors are on the back panel of the block.

Coil current varies from 30 to 280A.

The power system for the anode magnet

The power system consists of 2 separate blocks: a power block and a block with the capacitor bank. The total capacity of the capacitor bank is 800mkF (200mkF/1000V, 4). The neon lamp, which indicates that voltage exists in the capacitors, is brought to the front panel of the block. The Xc power block connector is placed on the back panel. It is not necessary to take into consideration the power polarity of the capacitor bank.

The power block scheme is shown in Fig.28. According to the scheme the C1-C4 capacitors take a charge through the Q1 thyristor and the R2 limited resistor till the voltage tapped off from the R4, R5 dividers isn't on target with the voltage specified by the R22 resistor. At this moment the signal on thyristor control electrode equals to zero and the thyristor goes to the OFF state. The capacitor bank discharge takes place through the Q2 thyristor activated by the timer signal.

The D14 diode is designed for the current stretching. The current waveform in the load is shown in Fig.29. The waveform is tapped off at 0.2 Om in the R8 resistor and at 200 V (20marks) in the capacitor bank.

The R22 capacitor voltage control handle, the load current control connector (W1), the capacitor voltage indicator are on the front panel of the block .The 220 V power, the timer's cable and the load are joined up with X1 connector, The capacitor bank is joined up with the Xc connector. Both X1, Xc connectors are on the back panel of the block.

The capacitor bank voltage varies from 80 to 470 V. The peak current in the load plotted against the number of marks on the capacitor bank voltage indicator is shown in Table A1.

Table A1. The number of marks on the capacitor bank voltage indicator

Marks	5	10	20	30	40
Current (A)	8	16	32	48	64

Power supply for e-beam transport coil

The power system consists of 2 separate blocks: a power block and a block with the capacitor banc. The total capacity of the capacitor bank is 800mkF (200mkF/1000V, 4). The neon lamp, which indicates that voltage exists in the

capacitors, is brought to the front panel of the block. The Xc power block connector is placed on the back panel. It is not necessary to take into consideration the power polarity of the capacitor banc.

The power block scheme is shown in Fig.30. According to the scheme the C1-C4 capacitors take a charge through the Q1 thyristor and the R2 limited resistor till the voltage tapped off from the R4, R5 dividers isn't on target with the voltage specified by the R22 resistor. At this moment the signal on thyristor control electrode equals to zero and the thyristor goes to the OFF state. The capacitor bank discharge takes place through the Q2 thyristor activated by the timer signal.

The D14, D15 diodes are designed for preservation of energy accumulated in the transport coil.

The current waveform in the transport coil is shown in Fig.31. The current waveform is tapped from the R8 viewing current resistor (75mB/5A) at 200 V (20marks) in the capacitor bank.

The R22 capacitor voltage control handle, the load current control connector (W1), the capacitor voltage indicator are on the front panel of the block .The 220 V power and the timer's cable are joined up with X1 connector. The capacitor bank is joined up with the Xc connector. The load is joined up with the Xl connector. The X1, Xc, Xl connectors are on the back panel of the block.

The capacitor bank voltage varies from 80 to 470 V. The peak current in the load plotted against the number of marks on the capacitor bank voltage indicator is shown in Table A2.

Table A2. The number of marks on the capacitor bank voltage indicator

Marks	10	20	30	40
Current (A)	25	50	77.3	102

Power supply for the e-beam focusing coil

The power system consists of 2 separate blocks: a power block and a block with the capacitor banc. The total capacity of the capacitor bank is 800mkF (200mkF/1000V, 4). The neon lamp, which indicates that voltage exists in the capacitors, is brought to the front panel of the block. The Xc power block connector is placed on the back panel. It is not necessary to take into consideration the power polarity of the capacitor banc.

The power block scheme is shown in Fig.32. According to the scheme the C1-C4 capacitors take a charge through the Q1 thyristor and the R2 limited resistor till the voltage tapped off from the R4, R5 dividers isn't on target with the voltage specified by the R22 resistor. At this moment the signal on thyristor control electrode equals to zero and the thyristor goes to the OFF state. The capacitor bank discharge takes place through the Q2 thyristor activated by the timer signal.

The Q3 thyristor is designed for regeneration mode.

The current waveform in the transport coil is shown in Fig.33. The waveform is tapped off at 0.12 Om in the R8 resistor and at 100 V (10marks) in the capacitor bank.

The R22 capacitor voltage control handle, the load current control connector (W1), the capacitor voltage indicator are on the front panel of the block .The 220 V power, the timer's cable and the load are joined up with X1 connector, The capacitor bank is joined up with the Xc connector. Both X1, Xc connectors are on the back panel of the block.

The capacitor bank voltage varies from 80 to 470 V. The peak current in the load plotted against the number of marks on the capacitor bank voltage indicator is shown in Table A3.

Table A3. The number of marks on the capacitor bank voltage indicator

Marks	10	20	30	40
Current (A)	45	89.6	128	168

The power system for the electron plasma emitter discharge

The system consists of a LC-line, which takes a charge from the BP-140 pomp power block and throws of the charge into the load through the SCR valve. The principal electric circuit is shown in Fig.34.

The K75-15 capacitors are used to assemble the LC-line. The inductance of the LC-line is reeled up on the unified former. There are 11 cells in the LC-line. The LC-line wave resistance (ρ) is 12 Om.

The TB 200-9 thyristors are used to assemble the SCR valve. The neon lamps indicating serviceability and equalizing circuits of MLT-2 resistors are placed parallel to the thyristors.

The actuation pulses come to the thyristors through the isolating transformers. The prime winding of the transformers is the loop of the RC- cable without braid. The loop is connected with the actuation block. According to the passport the cable insulation is worked out for 10kV of the direct voltage min.

To coordinate the LC-line resistance and the load resistance, the load circuit incorporates an additional resistance without inductance (R5, R6). The R7 resistance is used for LC-line discharge in case the break-through in the e-gun does not take place. The C12 capacitor is used to generate the anod-katod break-through voltage. At the first moment after the actuation the C12 capacitor can take a double voltage charge of the LC-line.

The starting block is a standard scheme of the capacitor discharge into the load (in our case it is a loop) through the inductance.

The "Power" handle and the lamp indicating the thyristor serviceability is on the front panel of the block. The loop is joined up to the X1 connector (A0, A9-A3; C0, C9-C3). The supply line and the timer's cable are joined up to the X2 connector (A9, C9; A2, C2). Both connectors are on the back panel of the block.

The current waveform tapped off the measuring resistor (CHC 75-50-0.5) in the real load at 6 kV in the capacitors is shown in Fig.35. The flat pulse peak current is 213 A. The pulse duration (on the base) is 130 μc.

Shot pulse generator

The high-voltage shot pulse generator is used to force initiating strike in e-gun with plasma cathode and forming start-up pulse for arc current modulator. The modulator maintains an arc discharge during the time, which is, defined the value of LC-line.

The usage of the generator allows expand appreciably the range of amplitude of current pulse modulator in the direction of smaller values.

The principal electric circuit is shown in Fig.36. The C2, C3 capacitors discharge takes place through the Q1 thyristor activated by the timer signal to the prime winding of T1 transformer. The pulse in the secondary winding has negative polarity and its peak value is 10 kV. The T3 transformer is used for the resistive decoupling of the light receiver block and the Q1 thyristor.

The T1 pulse transformer consists of eight stand-alone windings. Each winding contains 30 turns. The method of windings connection allows getting the coefficient of transformation equal to eight.

The load circuit contains the R1, R2 resistors to limit discharge current. R7 resistor and T5 transformer are used to form and transmit signal for actuation of the SCR commutator of the arc current modulator.

The high voltage pulse wave- form is shown in Fig.37. The viewing divider with the total resistance 100 kOm was connected to the output of the block. The divider gives a 1000:1coutdown.